



Cell-free DNA from nail clippings as source of normal control for genomic studies in hematologic malignancies

by Melissa Krystel-Whittemore, Kseniya Petrova-Drus, Ryan N. Ptashkin, Mark D. Ewalt, JinJuan Yao, Ying Liu, Menglei Zhu, Jamal Benhamida, Benjamin Durham, Jyoti Kumar, Khedoudja Nafa, Iwona Kiecka, Anita S. Bowman, Erika Gedvilaite, Jacklyn Casanova, Yun-Te Lin, Abhinata S. Mohanty, Satshil Rana, Anoop Balakrishnan Rema, Ivelise Rijo, Nelio Chaves, Paulo Salazar, Anita Yun, Sean Lachhander, Wei Wang, Mohammad S. Haque, Wenbin Xiao, Mikhail Roshal, Sergio Giralt, Gilles Salles, Raajit Rampal, Eytan M. Stein, Miguel-Angel Perales, Steven Horwitz, Ann Jakubowski, Doris Ponce, Alina Markova, Ozge Birsoy, Diana Mandelker, Simon Mantha, Ahmet Dogan, Ryma Benayed, Marc Ladanyi, Michael F. Berger, A. Rose Brannon, Ahmet Zehir, Chad Vanderbilt, and Maria E. Arcila

Received: January 12, 2024.

Accepted: February 29, 2024.

Citation: Melissa Krystel-Whittemore, Kseniya Petrova-Drus, Ryan N. Ptashkin, Mark D. Ewalt, JinJuan Yao, Ying Liu, Menglei Zhu, Jamal Benhamida, Benjamin Durham, Jyoti Kumar, Khedoudja Nafa, Iwona Kiecka, Anita S. Bowman, Erika Gedvilaite, Jacklyn Casanova, Yun-Te Lin, Abhinata S. Mohanty, Satshil Rana, Anoop Balakrishnan Rema, Ivelise Rijo, Nelio Chaves, Paulo Salazar, Anita Yun, Sean Lachhander, Wei Wang, Mohammad S. Haque, Wenbin Xiao, Mikhail Roshal, Sergio Giralt, Gilles Salles, Raajit Rampal, Eytan M. Stein, Miguel-Angel Perales, Steven Horwitz, Ann Jakubowski, Doris Ponce, Alina Markova, Ozge Birsoy, Diana Mandelker, Simon Mantha, Ahmet Dogan, Ryma Benayed, Marc Ladanyi, Michael F. Berger, A. Rose Brannon, Ahmet Zehir, Chad Vanderbilt, and Maria E. Arcila.

Cell-free DNA from nail clippings as source of normal control for genomic studies in hematologic malignancies. *Haematologica*. 2024 Mar 7. doi: 10.3324/haematol.2024.285054 [Epub ahead of print]

Publisher's Disclaimer.

E-publishing ahead of print is increasingly important for the rapid dissemination of science. Haematologica is, therefore, E-publishing PDF files of an early version of manuscripts that have completed a regular peer review and have been accepted for publication. E-publishing of this PDF file has been approved by the authors. After having E-published Ahead of Print, manuscripts will then undergo technical and English editing, typesetting, proof correction and be presented for the authors' final approval; the final version of the manuscript will then appear in a regular issue of the journal. All legal disclaimers that apply to the journal also pertain to this production process.

Cell-free DNA from nail clippings as source of normal control for genomic studies in hematologic malignancies

Authors

Melissa Krystel-Whittemore¹⁺, Kseniya Petrova-Drus¹, Ryan N. Ptashkin¹⁺, Mark D. Ewalt¹, JinJuan Yao¹, Ying Liu¹, Menglei Zhu¹, Jamal Benhamida¹, Benjamin Durham¹, Jyoti Kumar¹, Khedoudja Nafa¹, Iwona Kiecka¹, Anita S. Bowman¹, Erika Gedvilaite¹, Jacklyn Casanova¹, Yun-Te Lin¹, Abhinata S. Mohanty¹, Satshil Rana¹, Anoop Balakrishnan Rema¹, Ivelise Rijo¹, Nelio Chaves¹, Paulo Salazar¹, Anita Yun¹, Sean Lachhander¹, Wei Wang¹, Mohammad S. Haque¹, Wenbin Xiao¹, Mikhail Roshal¹, Sergio Giralt², Gilles Salles², Raajit Rampal², Eytan M. Stein², Miguel-Angel Perales², Steven Horwitz², Ann Jakubowski², Doris Ponce², Alina Markova², Ozge Birsoy¹, Diana Mandelker¹, Simon Mantha², Ahmet Dogan¹, Ryma Benayed¹⁺, Marc Ladanyi¹, Michael F. Berger¹, A. Rose Brannon¹, Ahmet Zehir¹⁺, #Chad Vanderbilt¹ & #Maria E. Arcila¹

authors contributed equally to this work

Affiliations

1. Department of Pathology and Laboratory Medicine, Memorial Sloan Kettering Cancer Center, New York, NY, USA
2. Department of Medicine, Memorial Sloan Kettering Cancer Center, New York, NY, USA

+ current address:

MKW: Department of Pathology, NYU Langone Health, New York, NY USA

RNP: C2i Genomics, New York, NY, USA

RB and AZ: Precision Medicine and Biosamples, AstraZeneca, New York, NY USA

Correspondence: Maria Arcila, arcilam@mskcc.org

Authors' contributions: MEA, CV, RP, MFB, and MKW, reviewed, analyzed, interpreted data, and performed statistical analyses and conclusions. All authors read and reviewed manuscript and contributed to the review process.

Disclosures: MKW: AstraZeneca: Advisory board, speaker; Foundation Medicine: professional services. KPD has received an honorarium (not related to this study) from Invivoscribe, Inc., San Diego, CA. RNP is an employee of C2i Genomics. RR: Consulting Fees: Incyte Corporation, Celgene/BMS, Blueprint, Abbvie, CTI, Stemline, Galecto, Pharmaessentia, Constellation/Morphosys, Sierra Oncology/GSK, Cogent, Sumitomo Dainippon, Kartos, Servier, Zentalis, Karyopharm. Research Funding: Constellation pharmaceuticals, Ryvu, Zentalis and Stemline Therapeutics. MAP reports honoraria from Adicet, Allogene, Allovir, Caribou Biosciences, Celgene, Bristol-Myers Squibb, Equilium, ExeVir, ImmPACT Bio, Incyte, Karyopharm, Kite/Gilead, Merck, Miltenyi Biotec, MorphoSys, Nektar Therapeutics, Novartis, Omeros, OrcaBio, Sanofi, Syncopation, VectivBio AG, and Vor Biopharma. He serves on DSMBs for Cidara Therapeutics, Medigene, and Sellas Life Sciences, and the scientific advisory board of NexImmune. He has ownership interests in NexImmune, Omeros and OrcaBio. He has received institutional research support for clinical trials from Allogene, Incyte, Kite/Gilead, Miltenyi Biotec, Nektar Therapeutics, and Novartis. SH: Consulting: Affimed, Abcurio Inc, Corvus, Daiichi Sankyo, Kyowa Hakko Kirin, ONO Pharmaceuticals, SeaGen, SecuraBio, Takeda, Yingli. Research: ADC Therapeutics, Affimed, C4, Celgene, Crispr Therapeutics, Daiichi Sankyo, Dren Kyowa Hakko Kirin, Millennium /Takeda, Seattle Genetics, and, SecuraBio. DP reports honoraria from Incyte and Sanofi. She has served as advisory board for Evive Biotechnology (Shanghai) Ltd (formerly Generon [Shanghai] Corporation Ltd), Kadmon-Sanofi Corporation, Ceramedix, and Incyte. Has research funding from Incyte Corporation and Sanofi. AM receives research funding from AstraZeneca, Incyte Corporation, Kintara Therapeutics, and Amryt Pharma; consults for ADC Therapeutics, Alira Health, AstraZeneca, Protagonist Therapeutics, OnQuality, and Janssen; and receives royalties from UpToDate. SM: Principal owner of Daboia Consulting LLC. AD receives research support from Roche and Takeda. MFB: Consulting: Eli Lilly, AstraZeneca, Paige.AI. Research Support: Boundless Bio. Intellectual Property Rights: SOPHiA Genetics. CV: Equity, intellectual property rights, and professional services and activities for Paige AI, Inc. MEA: Speaker: Biocartis, Invivoscribe, physician educational resources (PER), Peerview institute for medical education, clinical care options, RMEI medical education. Consulting: Janssen Global Services, Bristol-Myers Squibb, AstraZeneca, Roche, Biocartis, Sanofi.

DATA AVAILABILITY

The minimal clinical and somatic alteration data (including mutations and allele-specific copy number calls) necessary to replicate the findings in the article have been deposited to <https://github.com/chadvanderbilt/Nails/tree/main/data>. Source data are provided. Raw sequencing data cannot be broadly available due to privacy laws; patient consent to deposit raw sequencing data was not obtained.

FUNDING

Supported by the Comprehensive Cancer Center Core Grant P30CA008748 at Memorial Sloan Kettering Cancer Center from the NIH.

Abstract

Comprehensive genomic sequencing is becoming a critical component in the assessment of hematologic malignancies, with broad implications for patient management. In this context, unequivocally discriminating somatic from germline events is challenging but greatly facilitated by matched analysis of tumor:normal pairs. In contrast to solid tumors, conventional sources of normal control (peripheral blood, buccal swabs, saliva) could be highly involved by the neoplastic process, rendering them unsuitable. In this work we describe our real-world experience using cell free DNA (cfDNA) isolated from nail clippings as an alternate source of normal control, through the dedicated review of 2,610 tumor:nail pairs comprehensively sequenced by MSK-IMPACT-heme. Overall, we find nail cfDNA is a robust source of germline control for paired genomic studies. In a subset of patients, nail DNA may have tumor DNA contamination, reflecting unique attributes of the hematologic disease and transplant history. Contamination is generally low level, but significantly more common among patients with myeloid neoplasms (20.5%; 304/1482) compared to lymphoid diseases (5.4%; 61/1128) and particularly enriched in myeloproliferative neoplasms with marked myelofibrosis. When identified in patients with lymphoid and plasma-cell neoplasms, mutations commonly reflected a myeloid profile and correlated with a concurrent/evolving clonal myeloid neoplasm. For nails collected after allogeneic stem-cell transplantation, donor DNA was identified in 22% (11/50). In this cohort, an association with recent history of graft-vs-host disease was identified. These findings should be considered as a potential limitation for the use of nail as normal control but could also provide important diagnostic information regarding the disease process.

Introduction

Hematologic malignancies constitute a diverse set of primarily myeloid and lymphoid neoplasms characterized by somatically acquired genetic alterations which promote cell survival and proliferation. Today, genetic characterization is a pivotal component of nearly every form of hematologic malignancy, with increasing roles in diagnosis, classification, prognostication, therapeutic decision-making and monitoring.

Due to the complexity and broad range of genetic alterations that may define each disease, next generation sequencing (NGS) has emerged as a more practical approach for upfront comprehensive assessment over existing low-throughput techniques. An inherent challenge of such studies lies in the ability to correctly distinguish somatically acquired (cancer specific) from germline alterations when using a tumor-only model. Paired studies, matching tumor, and normal samples, constitute a superior method that allows unequivocal determinations and enables more sophisticated and accurate analyses of genetic variants.

Blood, buccal swabs, and saliva are traditional sources of normal control for paired sequencing in solid tumors. Depending on the hematologic malignancy, however, these controls are unsuitable due to the presence of neoplastic cells at various levels. Nail clippings are an alternative source but their use in routine clinical practice has not been sufficiently explored.

In this study, we describe our experience using DNA derived from nail tissue. We describe our rapid protocol for extraction, performance characteristics and overall results based on the routine clinical sequencing of 2610 tumor:nail pairs with our hybrid capture MSK-IMPACT heme assay (Integrated Mutation Profiling of Actionable Cancer Targets for Hematologic malignancies). We further discuss the benefits and pitfalls and highlight unique findings using this tissue source.

Methods

Diagnostic tumor samples (blood, bone marrow, tumor biopsies) submitted for routine molecular profiling using MSK-IMPACT-heme were selected, specifically those submitted with nails as the normal control. Fingernail clippings were submitted following standard nail collection protocols described in the supplemental methods section. All patients provided informed consent for paired sequencing and the study was conducted following MSK Institutional Review Board approval. Relevant clinicopathologic information was retrieved from electronic medical records. Each diagnosis was confirmed by a board-certified hematopathologist and a molecular pathologist.

SAMPLE PREPARATION:

Tumor DNA was extracted using previously described protocols.(1) Nail DNA extraction used the QIAamp® DNA investigator kit (Qiagen) for forensic and human identity samples. Two nail fragmentation methods were used (Figure 1A): Method 1 strictly followed manufacturer's protocol. Briefly, nail clippings (2-3, ~10mg) were cut into 1-2mm fragments with scissors before overnight digestion in proteinase K. When undigested particles were present after overnight incubation, additional proteinase K was added, and the process was repeated for several cycles to allow complete digestion. In method 2, nail clippings (~10mg) were pulverized using a BeadBlaster™ tissue homogenizer (Benchmark Scientific, NJ) following adjusted bone tissue protocols (2, 3), detailed in the supplementary methods section. Method 1 was used clinically from January 2017 to June 2019 and method 2 from July 2019 to December 2021.

DNA concentration was measured by Qubit fluorometer using the dsDNA HS Assay kit (ThermoFisher Scientific/Invitrogen Cat. No. QC32854). Subsets were analyzed by the Agilent 5300 Fragment Analyzer System with the HS Small Fragment kit and the HS Genomic DNA Kit (Agilent, Santa Clara, CA) to assess fragment profiles, following manufacturer protocols.

SEQUENCING AND DATA ANALYSIS

Sequencing was performed by MSK-IMPACT Heme, a custom hybridization capture–based NGS assay for the detection of somatic mutations and copy number alterations in coding regions of 400 genes.(1) Library preparation, sequencing, variant calling, and annotation were performed using matched tumor:normal pair analysis pipelines as previously described.(1, 4-6) Donor DNA was also sequenced as a normal control in post-transplant cases. Variant calling was performed in paired-sample mode with manual curation, side-by-side with the corresponding results of the nail and donor sample (when applicable), at the same position. Final variant calling was performed in the context of the patient’s clinicopathologic history, incorporating information on annotated population frequencies, when necessary. When available, correlation with prior and subsequent samples was performed.

ANALYSIS OF NAIL SEQUENCING RESULTS

Somatic variants clinically reported in tumor samples were extracted from the database along with the variant allele frequencies (VAF’s) of the same alteration in the nail sample. Accompanying metadata was extracted, including depth of coverage at variant start site, OncoKB classification,(7) and variant class (e.g. indel, SNV, etc.). Nail mutations were called if the variant was detected at a VAF of $\geq 1\%$ with at least 5 supporting reads. Any alteration below this level was within our established level of noise for the assay and were filtered out.

STATISTICS

Statistical analysis was performed using R (version 4.1.1). Variables were analyzed using both paired and unpaired T tests, as applicable.

Results

EXTRACTION

A side-by-side comparison of the 2 methods was performed on a validation set (20 samples). Overall, method 2 had markedly shorter procedural time and improved yields. Method 1 required several digestion cycles (2-6days), compared to a single digestion cycle for method 2 (overnight). Mean DNA yields averaged 12.5ng/mg and 20.9ng/mg (1.7-fold increase) for methods 1 and 2, respectively.

Comparison of DNA fragment sizes was performed to determine the effect of mechanical pulverization. Using the 5300 Fragment Analyzer System with the HS Small Fragment kit, the average fragment length was 154 bp and 169 bp for methods 1 and 2, respectively (Figure 1B); the differences were not statistically significant by paired t-test ($p=0.16$). To further assess for the presence of larger fragments, a set of 17 samples processed with method 2 were randomly selected for analysis using the HS Genomic DNA Kit. In all cases, the dominant peak was observed to migrate between the 75 and 163bp range, at a modal length of 153bp. Variable presence of a second and/or third minor peaks was also observed, averaging 672 and 2021 bp (migration range ~550-900 and ~900-7000, respectively). Representative electropherogram is presented in Figure 1C.

CLINICAL COHORT

Between January 2017 and December 2021, 4,395 nail samples were received for extraction: 1,807 and 2,616 were processed by methods 1 and 2, respectively (includes 28 processed by both methods corresponding to the validation set and 8 samples repeated during method transition). For clinical testing, 2-3 clippings were routinely extracted without weight measurements. Total DNA yield was significantly lower for method 1 ($p<2.2e-16$), average 398.7 ng vs 835.4 ng with method 2 (Figure 1D). At initial extraction, 79.5% (1,438/1807) and 89% (2,329/2,616) of samples extracted with methods 1 and 2, respectively, met the minimum

optimal input for sequencing by our assay (50ng). Re-extraction of 83 samples with higher input rescued 68.7% (61.5%; 32/52 method 1 and 80.6%; 25/31 method 2).

SEQUENCING DATA

In total, 2610 unique tumor:normal pairs (2610 patients) were sequenced for initial characterization. Monitoring tumor samples from the same patient were excluded to avoid duplication. The median interval for collection of the nail and tumor sample was 3 days (Average 42 days; range -1512 days to +7042 days); 88% of nail clippings were collected within +/- 120 days of the tumor sampling. Outliers were related to retrospective sequencing of a remote tumor or use of an archived nail sample (Supplementary Table 1).

For nail samples, insert size distributions were significantly shorter for those processed with method 1 as detailed in Figure 1E. Mean targeted coverages were also lower, averaging 785X (range 100-1484, median 805, SD 245) for method 1, vs 948X for method 2 (range 126-2742, median 939, SD 312.2) ($p < 2.2e-16$). See typical insert size distribution and pattern of nails in Figure 1F.

In all, 10,942 somatic mutations were detected across tumors (4,640 and 6302 in myeloid and lymphoid disease categories, respectively). Of these, 792 (7.2%) were detected in the corresponding nails of 365 patients (13.9%; 365/2610). Mutations in nails were significantly more common among patients with myeloid neoplasms (20.5%; 304/1482) compared to lymphoid diseases (5.4%; 61/1128) ($p < 2.2e-16$). The overall patient distribution, according to broad disease categories, is presented in **Figures 2A & B, and Supplementary Table 2**. The average number of mutations per nail was 2 (range 1-12).

To further establish general trends, mutations were stratified by VAF's (Figure 2C). Tumor VAF's averaged 26.7% (range 1 to 99.7%); if present, nail mutations were detected at a significantly lower level ($p < 2.2e-16$), averaging 4.4% (range 1 to 57.9%). Absolute differences in VAF's (tumor vs nail) are depicted in Figures 2D-E; the distribution of individual events in tumor and corresponding nail are further detailed in Figures 3A-F. In 19 patients (0.7%; 19/2610), nail

mutations were detected at VAF's close to (<2 fold lower) and even slightly higher than the tumor sample, indicating high tumor contamination; details are outlined in Supplementary **Table 3**. In 3 cases, this could be attributed to gaps in collection, with nails collected at the time of highest disease burden and tumor at very low level in a sample provided after interim therapy (Figure 3G). Despite the contamination, determination of somatic vs germline was readily possible in all, except in a unique case represented in Figure 3H. Of note, among the myeloid neoplasms, mutations with the highest VAF's in the tumor were more likely to be detected in the nail DNA. By contrast, among lymphoid neoplasms, mutated genes with the highest VAF in tumor were not detected in nail samples, supporting that high tumor VAF alone does not drive the detection of mutations in the nail.

The most commonly mutated genes in tumors and nails are depicted in Figures 4A and 4B. Mutations in nails were overwhelmingly biased to genes frequently altered in myeloid neoplasms in the myeloproliferative neoplasm (MPN) and myelodysplastic syndrome (MDS) spectrum. While observed VAF's in nails generally remained below 5%, alterations in *TET2*, *JAK2*, *ASXL1*, *DNMT3A*, *SRSF2* and *MPL* exhibited the highest number of outliers (Figure 4C). Prevalent pathologic features across cases with mutations at VAF's >5% (seen in 92 patients, 3.5% of total cohort) included the presence of marked bone marrow fibrosis and osteosclerosis (33%, 31/92), and myeloid neoplasms with monocytic features (13%, 12/92). Mutations with the highest VAF's also corresponded to genetic alterations with loss of heterozygosity (LOH). Representative cases are depicted in Figure 4D.

Notably, among the lymphoid and plasma cell neoplasms, common recurrent mutations in genes such as *BRAF*, *MYD88*, *IDH2*, *RHOA*, *IDH2*, *CREBBP*, *EP300* and others were distinctly absent in nails. Instead, 45% (53/118) of nail mutations overlapped with the most commonly described for myeloid neoplasms. While a full work up was not possible in all cases, in selected patients (primarily those with nail mutations with VAF's above 3%), it could be determined that the patients had an emerging or coexisting clonal myeloid process with only mutations of myeloid origin identified in the nail. Selected case studies are depicted in Figures 5A-C. Among the patients with T cell lymphomas and mutations in the nails, 3 had documented cutaneous

involvement, together harboring 22 mutations, 32% of all mutations detected in the subset (22/69). Despite the high number of mutations, all were detected at low level, between 1-2% VAF.

POST-TRANSPLANT NAIL SAMPLES

In all, 51 nail samples were collected after HCT, at an average interval of 834 days (range 3 to 3,918). Single nucleotide polymorphism (SNP) profiles of tumor, donor and nail samples were compared to determine the presence of donor component in the nail. A subset (n=27) was also tested using standard short tandem repeat (STR) analysis for chimerism assessment. Results are summarized in Supplementary Table 4. Of the 50 samples successfully analyzed, 78.3% (39/50) were 100% host and 22% (11/50) chimeric mostly host; donor component ranged from 5 to 42%. There was no correlation between the presence and/or degree of donor component and the length of time since transplant. In this cohort, a history of active GVHD (within 5 months prior to nail sampling) was significantly higher among patients with donor DNA in the nail (63.6%; 7/11) compared to all host (15.4%; 6/39) ($p=0.001$).

Discussion

Routine paired tumor-normal sequencing has undeniable advantages in clinical genomics. This approach is ideal at many levels, not only for the unambiguous determination of somatic versus germline variants but also to facilitate the assessment of LOH and second-hits in tumors, detect copy number alterations with higher sensitivity, estimate tumor mutation burden and mutational signatures more reliably, and to enable laboratory quality control (QC) checks related to sample identity. In previous studies we have shown that this can be successfully performed at a large scale in the clinical setting, both for solid (4, 8, 9) and liquid tumors.(1) The overall approach, however, proves to be more complex with hematologic malignancies, where alternate sources of normal DNA must be explored. In this report, we concentrated on the use of nails as a unique source of DNA that is rarely utilized in clinical practice. To our knowledge,

this is the largest and first study to describe its use for routine clinical comprehensive genomic testing.

The use of DNA from nails has been documented for over 30 years.(10-16) Historically, however, reports have remained scant and primarily confined to archeologic, forensic, and epidemiologic applications.(17-21) In the cancer molecular diagnostics setting, our clinical laboratory has accumulated over 20 years of experience using nails for matched tumor:normal testing.(22, 23) Overall, while generally considered an excellent source of germline DNA, major limitations to widespread use relate to the labor intensiveness of the extraction process and the scant/fragmented nature of the nucleic acid recovered. Biologically, nail DNA is a form of cell free DNA (cfDNA) that originates from germinal matrix cells at the nail root.(24, 25) During nail formation and growth, matrical cells mature and keratinize to ultimately form the structure of the nail plate. Through the keratinization phase, the cells undergo programmed cell death and release fragmented DNA that remains embedded in the surrounding keratinous matrix. In contrast to cfDNA in body fluids, the water-free environment of nail matrix protects the DNA from rapid cytosine hydrolytic deamination damage or oxidant degradation, rendering it viable for decades.(26) Both the matrix and nail bed are highly vascularized, such that the nail plate may be influenced by, and incorporate, elements from circulation.(27) Further, fingernails take approximately 3–6 months in healthy patients to grow from the germinal matrix to the free edge and, therefore, the DNA captured from nail clippings constitutes a record of up to 6 months of previous growth, and may be longer in patients with underlying malignancy, poor nutritional state, and/or receiving anticancer therapies.

Several nail DNA extraction methods have been investigated in the past, (13, 19) all involving cutting the nails into small fragments, followed by chemical lysis. Reported yields vary broadly, influenced by both biologic and technical heterogeneity (size of the cut fragments, duration, and type of chemical lysis). Here, we outlined our optimized clinical extraction protocol, which incorporates mechanical bead pulverization. In addition to circumventing cumbersome cutting procedures, chemical digestion time is markedly reduced from days to hours, which is critical to enable testing in a clinically actionable time. With this new method, average yields are also

improved and above the highest reported, after adjusting for expected differences in DNA measurement methods.

We confirm that DNA recovered from nail tissue is highly fragmented, and in keeping with degraded cfDNA. This has specific implications for testing, posing limitations on methods that require long fragments. However, we find the DNA to be high performing for hybrid-capture-based NGS assays as well as PCR-based assays of short amplicons. In contrast to cfDNA from plasma, the insert size distribution of nail cfDNA exhibits a prominent jagged or sawtooth pattern with 10bp periodicity. Similar findings were recently reported on sheared NGS libraries of 5 nail samples by Kakadia et al.(20) We postulate that this relates to specific and differential roles of DNases in nail tissue. In plasma, for instance, typical cfDNA fragment profiles primarily reflect the effect of DNASE1L3.(28) DNASE1 can further degrade DNA into shorter fragments with similar 10 bp periodicity, originating from digestion products of nucleosomes, which correspond to the 10 bp-per-turn structure of the DNA helix.(29) While this is not prominent in plasma, it is reported in urine where DNASE1 activity is much higher.(30) In nail, degradation of endogenous DNA during cornification of keratinocytes is orchestrated by DNase1L2(31) and may be responsible for this prominent pattern. Overall, the characteristic pattern suggests the protection of DNA from degradation by association with histones.

Our use of nail tissue in routine sequencing of hematologic malignancies highlighted important aspects of clinical utility that should be considered when implementing this control. One is that tumor contamination may be present in nail DNA in a small proportion of cases (13.9% in our cohort) and is distinctly biased toward the myeloid neoplasms. Importantly, in the overwhelming majority of cases, mutations were detected at low level, (98.5% at VAFs below 10% and 71.4% below 2%) or at significantly lower VAF's compared to the corresponding tumor, such that discrimination of the somatic vs germline nature of the variant was not compromised. Notably, VAF's above 20% were rare, seen in 0.4% of patients (13/2610), and over-represented in MPN with extensive marrow myelofibrosis and osteosclerosis and which harbored mutations in genes affected by LOH. We hypothesize that, in this context, the high contribution of tumor DNA in nail arises from a high turn-over of circulating hematopoietic

components in patients with extensive extramedullary hematopoiesis. The complications that occur in the natural history of patients with myelofibrosis, including both thrombotic and hemorrhagic events, may lead to entrapment of neoplastic cells in distal vascular locations, including the nail bed, where the DNA may become incorporated in the nail plate sampled. Contributing factors could also relate to adverse drug effects in skin and nail, such as hydroxyurea, (21) dietary factors and comorbidities.

While the causes of tumor DNA contamination in nail tissue remain to be defined, and are likely multifactorial in nature, the identification of the same common mutations across diseases, which also overlap with those seen in clonal hematopoiesis (CH), could support the roles of inflammation, ongoing microvascular damage and increased risk of thrombohemorrhagic events as recently highlighted in numerous CH publications.(32, 33) For instance, commonly mutated genes in CH, AML, MDS and MPN [*TET2*, *JAK2*, *ASXL1*, *DNMT3A*, *SF3B1* and *SH2B2*] have been associated with relative increases in platelet count and/or function and are implicated in the development of cardiovascular disease and thrombotic complications of both microvascular and macrovascular types.(34, 35) Both thrombotic and hemorrhagic effects in the nail bed microvasculature could promote the release of tumor DNA as described above.

Among patients with lymphoid neoplasms, the relative paucity of nail mutations was unexpected, particularly in the context of T-cell lymphomas with cutaneous involvement. Mutations detected, and particularly those identified at VAF $\geq 2\%$ (across B, T, and plasma cell neoplasms), were noteworthy by their overlapping profiles and frequent association with synchronous or rapidly evolving myeloid neoplasms. In these cases, lymphoid-specific mutations were distinctly absent, serving as a discrete clue of a separate myeloid clonal process. It should be mentioned that, among T-cell lymphomas (particularly angioimmunoblastic T-cell lymphoma (AITL) and T_H follicular helper cell), *TET2* and *DNMT3A* mutations are common alterations which can be shared across the T and myeloid compartments in approximately 70% of patients(36-38), consistent with a common stem cell progenitor that may give rise to distinct neoplasms (~20%), highlighting prominent roles of CH in the development of both diseases. The presence of CH-type mutations across nail samples

also raised the question of the role of chronicity and higher likelihood for tumor contamination due to extended exposure. While we cannot rule out a contribution, the presence of only CH-type mutations, even in largely chronic lymphoid neoplasms such as CLL/SLL, would argue against it and seems to support a distinct biologic behavior of these clonal populations.

Finally, the identification of donor DNA in nail clippings after allogeneic HCT has important implications for the use of nails as normal controls. Although literature remains scant, this finding has been previously documented. Results from 2 studies(39-41) (together 71 patients) have reported high variability in the incidence (43 to 100% of patients), proportion of donor component (4-95%) and even across fingernails of the same individual. While the reason remains unclear, possible mechanisms have been proposed which extrapolate from findings in other organ systems (donor cells in liver, lung, and others(42-44)), including donor hematopoietic stem cell conversion into non-hematopoietic cells and horizontal DNA transfer. (45-54) A potential etiology we also consider is graft versus host disease (GVHD). While documented or overt findings in nails or skin were not consistently present on review of medical records, the higher incidence of the donor component among patients with a history of GVHD within 5 months of sampling (the timeframe captured in a nail clipping) could support an active role and may reflect a systemic effect not necessarily evident on physical exam. Similar to what is seen among non-transplanted patients with myeloid neoplasms, mechanistically, it seems plausible that graft action on skin and distal vessels of the nail bed can lead to similar release of donor DNA that can be incorporated and detected in the clippings of the host nail plate. Further studies are required to better define this. Overall, however, and in the context of the central aspect of this work, it is important to qualify the suitability of the nail as a control by determining the presence and degree of chimerism. This may be done by short tandem repeat analysis prior to NGS testing. Alternatively, if the donor sample is also sequenced and the design of the assay allows, SNP analysis may also be performed. If there is minimal donor contamination, sequencing nail DNA in conjunction with the donor can be highly informative when analyzing data from difficult post-transplant samples.

Conclusions

In this report, we outline our experience using nail cfDNA as a “normal” control in comprehensive clinical genomic testing. While our findings support nail cfDNA as a highly valuable and informative source of DNA for paired studies, in a small subset of patients, nails reflect the patient’s hematologic disease and transplant history. This should be considered as a potential limitation, but it could also be exploited as a potential diagnostic tool to inform undiagnosed disease. Through the analysis of our data and search of the limited literature available, it is evident that our understanding of key facets of the biology of nail and the interaction with the hematopoietic system remains poor, leaving many questions of practical and academic interest to be answered. Closer clinical and pathologic assessment of nails in patients with hematologic diseases would enable further dedicated studies.

References

1. Ptashkin RN, Ewalt MD, Jayakumaran G, et al. Enhanced clinical assessment of hematologic malignancies through routine paired tumor and normal sequencing. *Nat Commun.* 2023;14(1):6895.
2. Kontopoulos I, Penkman K, Mullin VE, et al. Screening archaeological bone for palaeogenetic and palaeoproteomic studies. *PLoS One.* 2020;15(6):e0235146.
3. Kontopoulos I, Presslee S, Penkman K, Collins M. Preparation of bone powder for FTIR-ATR analysis: The particle size effect. *Vibr Spectrosc.* 2018:167-177.
4. Zehir A, Benayed R, Shah RH, et al. Mutational landscape of metastatic cancer revealed from prospective clinical sequencing of 10,000 patients. *Nat Med.* 2017;23(6):703-713.
5. Cheng DT, Mitchell TN, Zehir A, et al. Memorial Sloan Kettering-Integrated Mutation Profiling of Actionable Cancer Targets (MSK-IMPACT): A Hybridization Capture-Based Next-Generation Sequencing Clinical Assay for Solid Tumor Molecular Oncology. *J Mol Diagn.* 2015;17(3):251-264.
6. Shen R, Seshan VE. FACETS: allele-specific copy number and clonal heterogeneity analysis tool for high-throughput DNA sequencing. *Nucleic Acids Res.* 2016;44(16):e131.
7. Chakravarty D, Gao J, Phillips SM, et al. OncoKB: A Precision Oncology Knowledge Base. *JCO Precis Oncol.* 2017;2017:PO.17.00011.
8. Frampton GM, Fichtenholtz A, Otto GA, et al. Development and validation of a clinical cancer genomic profiling test based on massively parallel DNA sequencing. *Nat Biotechnol.* 2013;31(11):1023-1031.
9. Wagle N, Berger MF, Davis MJ, et al. High-throughput detection of actionable genomic alterations in clinical tumor samples by targeted, massively parallel sequencing. *Cancer Discov.* 2012;2(1):82-93.
10. Berglund EC, Kiialainen A, Syvänen AC. Next-generation sequencing technologies and applications for human genetic history and forensics. *Investig Genet.* 2011;2:23.
11. Krskova-Honzatkova L, Sieglova Z. Fingernail DNA: A suitable source of constitutional DNA in leukemia. *Lab Hematol.* 2000;6:145-146.
12. Matsuzawa N, Shimozato K, Natsume N, Niikawa N, Yoshiura K. A novel missense mutation in Van der Woude syndrome: usefulness of fingernail DNA for genetic analysis. *J Dent Res.* 2006;85(12):1143-1146.
13. Nakashima M, Tsuda M, Kinoshita A, et al. Precision of high-throughput single-nucleotide polymorphism genotyping with fingernail DNA: comparison with blood DNA. *Clin Chem.* 2008;54(10):1746-1748.
14. Park J, Liang D, Kim JW, et al. Nail DNA and possible biomarkers: a pilot study. *J Prev Med Public Health.* 2012;45(4):235-243.
15. Tanigawara Y, Kita T, Hirono M, Sakaeda T, Komada F, Okumura K. Identification of N-acetyltransferase 2 and CYP2C19 genotypes for hair, buccal cell swabs, or fingernails compared with blood. *Ther Drug Monit.* 2001;23(4):341-346.
16. van Breda SG, Hogervorst JG, Schouten LJ, et al. Toenails: an easily accessible and long-term stable source of DNA for genetic analyses in large-scale epidemiological studies. *Clin Chem.* 2007;53(6):1168-1170.
17. Hogervorst JG, Godschalk RW, van den Brandt PA, et al. DNA from nails for genetic analyses in large-scale epidemiologic studies. *Cancer Epidemiol Biomarkers Prev.* 2014;23(12):2703-2712.
18. Truong L, Park HL, Chang SS, et al. Human Nail Clippings as a Source of DNA for Genetic Studies. *Open J Epidemiol.* 2015;5(1):41-50.
19. Preuner S, Danzer M, Pröll J, et al. High-quality DNA from fingernails for genetic analysis. *J Mol Diagn.* 2014;16(4):459-466.

20. Kakadia PM, Van de Water N, Browett PJ, Bohlander SK. Efficient identification of somatic mutations in acute myeloid leukaemia using whole exome sequencing of fingernail derived DNA as germline control. *Sci Rep.* 2018;8(1):13751.
21. Malato A, Rossi E, Palumbo GA, Guglielmelli P, Pugliese N. Drug-Related Cutaneous Adverse Events in Philadelphia Chromosome-Negative Myeloproliferative Neoplasms: A Literature Review. *Int J Mol Sci.* 2020;21(11):3900.
22. Barbashina V, Salazar P, Holland EC, Rosenblum MK, Ladanyi M. Allelic losses at 1p36 and 19q13 in gliomas: correlation with histologic classification, definition of a 150-kb minimal deleted region on 1p36, and evaluation of CAMTA1 as a candidate tumor suppressor gene. *Clin Cancer Res.* 2005;11(3):1119-1128.
23. Barbashina V, Salazar P, Ladanyi M, Rosenblum MK, Edgar MA. Glioneuronal tumor with neuropil-like islands (GTNI): a report of 8 cases with chromosome 1p/19q deletion analysis. *Am J Surg Pathol.* 2007;31(8):1196-1202.
24. Eckhart L, Lippens S, Tschachler E, Declercq W. Cell death by cornification. *Biochim Biophys Acta.* 2013;1833(12):3471-3480.
25. de Berker DA, André J, Baran R. Nail biology and nail science. *Int J Cosmet Sci.* 2007;29(4):241-275.
26. Bengtsson CF, Olsen ME, Brandt L, et al. DNA from keratinous tissue. Part I: hair and nail. *Ann Anat.* 2012;194(1):17-25.
27. de Berker D. Nail anatomy. *Clin Dermatol.* 2013;31(5):509-515.
28. Han DSC, Ni M, Chan RWY, et al. The Biology of Cell-free DNA Fragmentation and the Roles of DNASE1, DNASE1L3, and DFFB. *Am J Hum Genet.* 2020;106(2):202-214.
29. Klug A, Lutter LC. The helical periodicity of DNA on the nucleosome. *Nucleic Acids Res.* 1981;9(17):4267-4283.
30. Xie T, Wang G, Ding SC, et al. High-resolution analysis for urinary DNA jagged ends. *NPJ Genom Med.* 2022;7(1):14.
31. Fischer H, Scherz J, Szabo S, et al. DNase 2 is the main DNA-degrading enzyme of the stratum corneum. *PLoS One.* 2011;6(3):e17581.
32. Avagyan S, Zon LI. Clonal hematopoiesis and inflammation - the perpetual cycle. *Trends Cell Biol.* 2023;33(8):695-707.
33. Marnell CS, Bick A, Natarajan P. Clonal hematopoiesis of indeterminate potential (CHIP): Linking somatic mutations, hematopoiesis, chronic inflammation and cardiovascular disease. *J Mol Cell Cardiol.* 2021;161:98-105.
34. Olivi M, Di Biase F, Lanzarone G, et al. Thrombosis in Acute Myeloid Leukemia: Pathogenesis, Risk Factors and Therapeutic Challenges. *Curr Treat Options Oncol.* 2023;24(6):693-710.
35. Papageorgiou L, Elalamy I, Vandreden P, Gerotziafas GT. Thrombotic and Hemorrhagic Issues Associated with Myeloproliferative Neoplasms. *Clin Appl Thromb Hemost.* 2022;28:10760296221097969.
36. Lewis NE, Petrova-Drus K, Huet S, et al. Clonal hematopoiesis in angioimmunoblastic T-cell lymphoma with divergent evolution to myeloid neoplasms. *Blood Adv.* 2020;4(10):2261-2271.
37. Nann D, Fend F, Quintanilla-Martinez L. [TFH lymphoma and associated clonal hematopoiesis]. *Pathologie (Heidelb).* 2023;44(Suppl 3):144-149.
38. Cheng S, Zhang W, Inghirami G, Tam W. Mutation analysis links angioimmunoblastic T-cell lymphoma to clonal hematopoiesis and smoking. *Elife.* 2021;10:e66395.
39. Imanishi D, Miyazaki Y, Yamasaki R, et al. Donor-derived DNA in fingernails among recipients of allogeneic hematopoietic stem-cell transplants. *Blood.* 2007;110(7):2231-2234.

40. Sanz-Piña E, Santurtún A, Freire J, Gómez-Román J, Colorado M, Zarrabeitia MT. The genetic profile of bone marrow transplant patients in different samples of forensic interest. *Forensic Sci Med Pathol*. 2019;15(2):178-183.
41. Robesova B, Drncova M, Folta A, et al. Donor-derived DNA variability in fingernails of acute myeloid leukemia patients after allogeneic hematopoietic stem cell transplantation detected by direct PCR. *Bone Marrow Transplant*. 2020;55(6):1021-1022.
42. Suratt BT, Cool CD, Serls AE, et al. Human pulmonary chimerism after hematopoietic stem cell transplantation. *Am J Respir Crit Care Med*. 2003;168(3):318-322.
43. Alison MR, Poulsom R, Jeffery R, et al. Hepatocytes from non-hepatic adult stem cells. *Nature*. 2000;406(6793):257.
44. Bittner RE, Schöfer C, Weipoltshammer K, et al. Recruitment of bone-marrow-derived cells by skeletal and cardiac muscle in adult dystrophic mdx mice. *Anat Embryol (Berl)*. 1999;199(5):391-396.
45. Waterhouse M, Themeli M, Bertz H, Zoumbos N, Finke J, Spyridonidis A. Horizontal DNA transfer from donor to host cells as an alternative mechanism of epithelial chimerism after allogeneic hematopoietic cell transplantation. *Biol Blood Marrow Transplant*. 2011;17(3):319-329.
46. Jang YY, Collector MI, Baylin SB, Diehl AM, Sharkis SJ. Hematopoietic stem cells convert into liver cells within days without fusion. *Nat Cell Biol*. 2004;6(6):532-539.
47. Terada N, Hamazaki T, Oka M, et al. Bone marrow cells adopt the phenotype of other cells by spontaneous cell fusion. *Nature*. 2002;416(6880):542-545.
48. Metaxas Y, Zeiser R, Schmitt-Graeff A, et al. Human hematopoietic cell transplantation results in generation of donor-derived epithelial cells. *Leukemia*. 2005;19(7):1287-1289.
49. Spyridonidis A, Schmitt-Gräff A, Tomann T, et al. Epithelial tissue chimerism after human hematopoietic cell transplantation is a real phenomenon. *Am J Pathol*. 2004;164(4):1147-1155.
50. Tran SD, Pillemer SR, Dutra A, et al. Differentiation of human bone marrow-derived cells into buccal epithelial cells in vivo: a molecular analytical study. *Lancet*. 2003;361(9363):1084-1088.
51. Spyridonidis A, Zeiser R, Follo M, Metaxas Y, Finke J. Stem cell plasticity: the debate begins to clarify. *Stem Cell Rev*. 2005;1(1):37-43.
52. Jiang Y, Jahagirdar BN, Reinhardt RL, et al. Pluripotency of mesenchymal stem cells derived from adult marrow. *Nature*. 2002;418(6893):41-49.
53. Takahashi K, Yamanaka S. Induction of pluripotent stem cells from mouse embryonic and adult fibroblast cultures by defined factors. *Cell*. 2006;126(4):663-676.
54. Halicka HD, Bedner E, Darzynkiewicz Z. Segregation of RNA and separate packaging of DNA and RNA in apoptotic bodies during apoptosis. *Exp Cell Res*. 2000;260(2):248-256.

Figure Legends

Figure 1: Summary of extraction methods and DNA quality characteristics.

A: Description of the 2 nail processing methods. Nail clippings were manually cut with scissors into small fragments (method 1) or pulverized (method 2), followed by enzymatic digestion and DNA extraction. Processing by method one takes several days for digestion (up to 6 days) compared to method 2 (<24 hours, generally overnight).

B. Comparison of fragment sizes obtained from method 1 and method 2 established using the 5300 Fragment Analyzer system with the HS small fragment kit. The average sizes were 154 bp and 169 bp for methods 1 and 2, respectively. Differences were not statistically significant ($p=0.16$).

C. Representative electropherogram showing the DNA fragment distribution obtained from a nail sample analyzed by the Agilent 5300 Fragment Analyzer System with the HS Genomic DNA Kit. DNA is primarily composed of short fragments with a main peak centered around 150 bp; highest point at 153 bp. Note that the presence of high molecular weight (HMW) DNA (arrow) represents a minimal proportion of the total DNA.

The numbers across the x and y axis are relabeled with larger characters over the original electropherogram to facilitate viewing.

D. Comparison of total DNA yields in nanograms (ng) observed across 4,356 nail DNA examples extracted between Jan 2017 and Dec 2021, stratified by method type; 1,807 and 2,616 were processed by methods 1 and 2, respectively. Average total DNA yields (Qubit measurements) were significantly lower for method 1, 398.7 ng (Min: 1.3, Median: 184.8, Max: 6,240.0), compared to method 2, 835.4 ng (Min: 1.2, Median: 470.4, Max: 9540.0). Method labeled on the x axis and total DNA yield denoted on the y axis. Overall distribution for method 1 and 2 is depicted on the right section and zoomed detail on the left. Differences are statistically significant ($p<2.2e-16$).

E. Comparison of insert sizes from sequenced libraries (sheared) of samples processed with the 2 methods. Insert sizes for each sample were divided by size and stratified into quartiles. Overall, samples processed by method 1 have a higher proportion of shorter inserts with statistically significant differences ($p < 0.001$) as compared to samples processed with method 2, suggesting higher degradation. Method 1 (mean 118 bp, range 41-176, SD 17.6) compared to method 2 (mean 126, range 59-200, SD 20.0)

F. Representative insert distribution plot including several clinical samples. Library insert sizes on the x axis and density (proportion of total) on the y axis. Note nail DNA exhibits a prominent jagged or sawtooth pattern with 10 bp periodicity in fragments below 150 pb. This is seen across all nail samples (sheared and non-sheared) but is most prominent in samples processed with method 1 after several days of digestion. Contrast to the pattern observed on sheared bone marrow DNA.

Abbreviations: bp=base pairs; ns=no statistical significance; RFU= Relative Fluorescence Unit
**** denotes statistically significant differences

Source data are provided as a Source Data file.

Figure 2: Distribution of patients and mutations by disease categories

A. Distribution of patients in the clinical cohort. Patients are categorized by broad disease category (OncoTree Classification System) as specified on the far left (y axis). For each category, the number of patients is denoted inside the parenthesis (n=patients with mutations in nail/total number of patients). Percent of patients on the x axis. Yellow bar depicts the proportion of patients with mutations in the nail; the blue bar depicts those patients with mutations identified only in tumor. The highest proportion of patients with mutations in the nail include MCD, MDS/MPN and MPN.

Abbreviations: Acute Leukemias of Ambiguous Lineage (ALAL), acute myeloid leukemias (AML), Blastic Plasmacytoid Dendritic Cell Neoplasm (BPDCN), Histiocytic and Dendritic Cell Neoplasms (HDCN), Mast cell diseases (MCD), Myelodysplastic Syndromes (MDS), Myelodysplastic/Myeloproliferative Neoplasms (MDS/MPN), Myeloid/Lymphoid Neoplasms with Eosinophilia and Rearrangement of *PDGFRA/PDGFRB* or *FGFR1* or with *PCM1-JAK2* (MLNER), Myeloproliferative Neoplasms (MPN), B-Lymphoblastic Leukemia/Lymphoma, Hodgkin Lymphoma (HL), Lymphoid Atypical (LATL), Mature B-Cell Neoplasms (MBN), Mature T and NK Neoplasms (MTNN), Plasma Cell Myeloma (PCM), T-Lymphoblastic Leukemia/Lymphoma. MDS and MPN work up denote cases with suspected MDS and MPN but work up was incomplete.

B. Distribution of mutations in the clinical cohort. The number of mutations is categorized according to the same broad OncoTree categories in A. For each category, the number of mutations is specified inside the parenthesis (n=mutations identified in nail/mutations in tumor only). The percent of mutations is depicted in the x axis. Yellow bar depicts the proportion of mutations identified in the nail; the blue bar corresponds to mutations identified only in the tumor. Diseases with the highest proportion of mutations identified in the nail include MPN, MDS/MPN and MCD.

C. Distribution of mutations by VAF (%), binned on the y axis and number of mutations across the cohort on the x axis. Tumor mutations (blue bars) were distributed over a broad range with VAF's, averaging 26.7%. By contrast, mutations in nail were identified at significantly lower VAF ($p < 2.2e-16$), average 4.4%. VAF's of mutations in nail were significantly lower for lymphoid neoplasms (yellow) compared to myeloid (red), at 3.3% vs 4.9%, respectively ($p = 0.006$).

D&E. Density plots depicting the absolute differences in VAF's for mutations detected in the nail, compared to the same mutation in the corresponding tumor sample and stratified based on tumor category (Lymphoid vs. Myeloid). Mutations in nail are present at VAF's that are significantly lower VAF's compared to the same mutation in the corresponding tumor. The large absolute differences between the tumor and the nail, allow the determination that the

variant is somatic in origin. The median absolute differences for mutations in patients with lymphoid malignancies was 29%, compared to 35% for those with myeloid malignancies. Using non-parametric Wilcoxon Rank Sum test (Mann-Whitney U test), the differences in distribution of lymphoid vs Myeloid are statistically significant ($p=0.0097$). Source data are provided as a Source Data file.

Figure 3. Comparison of variant allele frequencies between tumor and nail

A, B & C. Distribution of mutations in patients with tumors in the myeloid category.

A. Bar graph depicting all mutations detected in the myeloid tumors (blue). Each bar constitutes 1 mutation. Nail mutations (orange) are plotted next to the corresponding mutation in the tumor. A total of 4,649 mutations were detected in the tumors. Of these, 674 (14.5%) were identified in the corresponding nails. Mutations in the nail are arranged by VAF from highest to lowest (range 1-59.7%). The subset of cases with nail mutations is expanded and reorganized by the corresponding VAF in the tumor, from highest to lowest, for comparison (zoomed area to the right). In all, 304 patients harbored the 674 mutations in the nail. Of these, 13 (4.3% of patients) had VAF above 20%. Despite tumor contamination in the nail, VAF's in the nail were significantly lower compared to the tumor such that distinction between somatic and germline variants could be made in all cases except in 1 patient (see details in 3H). Note that rare mutations are identified at slightly higher VAF compared to the tumor. This corresponded to tumor samples submitted immediately after treatment, at the time minimal residual disease, while the nail reflected contamination from several months prior when the disease was at high level.

B. Mutations in myeloid tumors are stratified by their VAF (%) and binned as depicted on the y axis. The number of mutations in each category is denoted on the x axis.

C. The proportion of mutations identified in the nail based on the VAF of the mutation in the corresponding tumors. VAF (%) of mutations in the tumor in the y axis. The proportion of the corresponding mutations identified in the nail (orange) in the x axis. Note that in the myeloid

category, the higher the variant allele frequency of the mutations in the tumor, the higher the proportion identified in the nail.

D,E,& F. Distribution of mutations in patients with tumors in the lymphoid category. D. Bar graph depicting all mutations detected in the lymphoid tumors (blue). Each bar constitutes 1 mutation. Nail mutations (orange) are plotted next to the corresponding mutation in the tumor. A total of 6303 mutations were seen in the patients with lymphoid tumors. Of these, 118 mutations (1.9%) were identified in the corresponding nails. Mutations in the nail are arranged by VAF from highest to lowest (range 1-17.4%). The set of cases with nail mutations is expanded and reorganized by the corresponding VAF in the tumor, from highest to lowest, for comparison (zoomed insert to the right). In all, 61 patients harbored the 118 mutations in the nail.

E. Mutations in lymphoid tumors are stratified by their VAF and binned as depicted on the y axis. The number of mutations in each category denoted on the x axis.

F. The proportion of mutations identified in the nail based on the VAF of the mutation in the corresponding tumors. VAF (%) of mutations in the tumor in the y axis. The proportion of the corresponding mutations identified in the nail (orange) denoted on the x axis. Note that, in contrast to the myeloid tumors, mutations with the highest VAF's in the tumor are not present in the nail.

G. Distribution of nail samples based on VAF's and the timing of sampling relative to the corresponding tumor. The median interval between nail and tumor sampling was 3 days (range 1,512 days before the tumor to 7,042 after the tumor). The number of days is displayed on the x axis. Large gaps between collection of the two samples often reflected different disease loads causing diagnostic difficulties.

H. Only case in the cohort of 2610 patients with mutations in the nail at ~60% (similar to tumor) raising the possibility of a germline event. Across the entire cohort, the highest variant allele frequencies were associated with patients with myeloproliferative neoplasms and marked myelofibrosis. In all cases, except this unique case, the VAFs in the tumor were comparatively higher (double), allowing discrimination of the mutation as somatic. In this case, the JAK2 mutation was detected ~60% in both tumor and normal. Per history, patient had trauma to the

hands and upper extremities associated with his job. Multiple hematomas and ecchymosis on the upper extremity were documented in the weeks prior to the nail collection. The finding of several other mutations at high level and the overall pattern suggested tumor contamination, likely related to trauma. Reticulin stain of a prior bone marrow biopsy shows 3+ fibrosis. Right table lists all mutations and corresponding VAF's in the blood sample in our cohort, the corresponding nail collected 4 months later and the subsequent blood sample after 2 years.

Figure 4. Most common alterations identified in nail DNA

A. Heatmap showing the distribution of mutated genes identified in the nails based on disease categories. Genes included are the most commonly mutated, defined as those altered with a frequency $>0.5\%$ among the total mutations in nails or tumor. In nails, this encompassed genes mutated >4 times among the 792 mutations detected; in tumor, this encompassed genes mutated >50 times among the 10,942 mutations. Mutated genes are organized based on frequency in the tumor, with the highest number of mutations at the top. The total number of mutations in each disease category is annotated in the first row, followed by details of the number of mutations in each gene by disease category. Boxes are color coded as indicated by the color scale (red) indicating the % or the total mutations that were identified in the nail.

B. Number of total mutations identified in each gene are listed in columns labeled Total Nail and Total Tumor. In the top row, all mutations detected in the cohort followed by detailed numbers in each gene. The proportion of total tumor mutations that are identified in the nail are displayed as a percentage at the far-right column (plotted as a side bar and labeled).

C. Most frequently mutated genes in nails across all disease categories in order of frequency from left to right (TET2 most common). Distribution of mutations by VAF (%) on the y axis. Although most mutations in these genes were identified in the nails at VAF below 10%, these genes also had the highest number of outliers, often related to the presence of Loss of heterozygosity (LOH).

D. Assessment of somatic copy number alteration profiles of 2 tumor samples demonstrate CN-LOH involving genes *TET2* (Chromosome 4) and *JAK2* (chromosomes 9). MSK-IMPACT heme analysis includes the assessment of genome-wide total and allele-specific copy number states which are calculated using the open-source R package FACETS2n (v0.3.0). The mutations were detected in the tumor at VAF's of 91% (*TET2*) and 89% (*JAK2*), respectively. The corresponding nail samples had the same mutations at VAF's of 40% and 36%, respectively.

Figure shows the integrated visualization of FACETS analysis. Top panels display total copy number log-ratio along genomic positions on chromosome 4 (left) and 9 (right), both copy neutral. Middle panels show the allele specific log-odds-ratio revealing allelic divergence for regions of chromosomes 4 (left) and 9 (right), consistent with loss of heterozygosity events. The bottom panel displays the inferred integer copy number with allelic losses of chromosomal segments 4 (left) and 9 (right) in the genomic regions containing *TET2* and *JAK2*, respectively (red lines). Black line corresponds to the total copy number.

Figure 5. Representative cases of lymphoma or plasma cell neoplasms with tumor mutations identified in nail DNA.

For A, B and C, the tables display the mutations detected in each sample sequenced, along with the corresponding VAF's (%), highlighted according to the color scale (top right). Myeloid (M) lineage mutations are highlighted in red. Lymphoid/plasma cell (L/PC) associated mutations are highlighted in blue. Samples appear in order of collection; time in parenthesis is the interval relative to sample 1.

A. 83-year-old male with history of chronic lymphocytic leukemia / small lymphocytic lymphoma (CLL/SLL) for 13 years, on active surveillance (known *BRAF*, *NRAS* and *KRAS* mutations). Presents for further assessment of suspected progression of disease (increased lymphocytosis, fatigue, anemia, and worsening thrombocytopenia). The blood sample (Bulk blood, 1) showed evidence of CLL/SLL, 59.4% by flow cytometry (FC). Sequencing revealed 13

mutations – The top 8 were consistent with the previously diagnosed CLL/SLL. Other mutations (red) suggested a coexisting myeloproliferative neoplasm. Only the latter subset was detected in the nail (2). A bone marrow (BM) sample (3) was obtained 2 weeks later, demonstrating a genomic profile identical to the blood. B and myeloid cell populations were sorted (4 and 5, respectively) and sequenced independently, showing segregation of the mutations into two distinct categories of lymphoid and myeloid origin. Morphologically (bottom left), the BM sample revealed extensive CLL/SLL (insert highlights ~80% involvement by PAX-5 immunostain). Bottom right shows areas with increased atypical megakaryocytes, severe reticulin fibrosis (insert shows retic stain), and no increase in blasts. The findings are consistent with a *JAK2* p.V617F and *MPL* p.W515L-Mutated Myeloproliferative Neoplasm, fibrotic phase of primary myelofibrosis (PMF) coexisting with CLL/SLL. Note that despite the known chronicity of the CLL and markedly higher VAF's for the lymphoid derived mutations, it is only the myeloid derived mutations that are identified in the nail.

B. 80-year-old female with a 2-year history of smoldering myeloma presents with progressive cytopenia. A BM sample is obtained (1) demonstrating patchy involvement by a plasma cell myeloma (PCM), ~15% by aspirate differential (2.9% of WBC by flow cytometry). No myelodysplasia is identified. Bulk BM sequencing revealed 6 mutations: one subclonal PRDM1 and 5 mutations at high VAF (*TET2*, *PHF6*, *CUX1* and *KMT2C*), the latter 5 detected in the nail sample (2). A subsequent BM sample (3) 1 year later showed increased patchy involvement by PCM (40-80% on aspirate differential, 20% by flow cytometry) and overt dysplastic changes, while sequencing demonstrated the same mutations previously detected. To further assess the myeloma component, plasma cells were isolated from an aliquot of the same sample (CD138 Magnetic Bead-based Positive Selection) and sequenced (4). This enriched population established the myeloma specific genomic profile, which excluded the 5 mutations detected in the nails. Further BM sampling 2 years later (5) showed overt multilineage dysplasia with a minimal plasma cell component (<5%). At this time the mutation profile reflected only the myeloid derived mutations. Table displays the

specific mutations detected in each sample. Bottom left picture depicts the findings of the BM sample (3), which is involved by both plasma cell neoplasm and Myelodysplastic syndrome (MDS). Note the dysplastic megakaryocytes among numerous plasma cells. CD138 immunostain highlights the plasma cells (bottom right). The overall findings are consistent with plasma cell neoplasm with an emerging MDS. Mutations detected in the nail DNA correspond to those detected in the myeloid neoplasm and preceded overt morphologic features of dysplasia. All plasma cell lineage mutations were distinctly absent in the nail DNA.

C. 71-year-old female with history of angioimmunoblastic T-cell lymphoma (AITL) presents with disease recurrence. Sequencing of DNA from an involved lymph node showed 10 mutations as detailed in the table (sample 1). Only a subset was detected in the nail DNA (2), specifically those associated with clonal hematopoiesis but hallmark mutations of AITL (*RHOA*, *IDH*) were distinctly absent. A blood sample (3) was obtained 6 months later, showing minimal involvement by an abnormal T cell population (0.060% of the WBC by FC). However, sequencing demonstrated the same mutations (CH type) identified in the nail, at very high level. A follow up BM sample 1 year later demonstrated minimal residual involvement by AITL (0.0043% of WBC by FC); morphologically the BM was markedly hypercellular with mild dyspoiesis. Sequencing revealed the 3 same mutations and emergence of a JAK2 mutation. In conjunction, the findings were consistent with a new myelodysplastic / myeloproliferative neoplasm emerging in a patient with active AITL. Bottom left picture depicts the involvement by AITL in the lymph node (insert shows cells highlighted by CD3 immunostaining). On the right, the markedly hypercellular bone marrow.

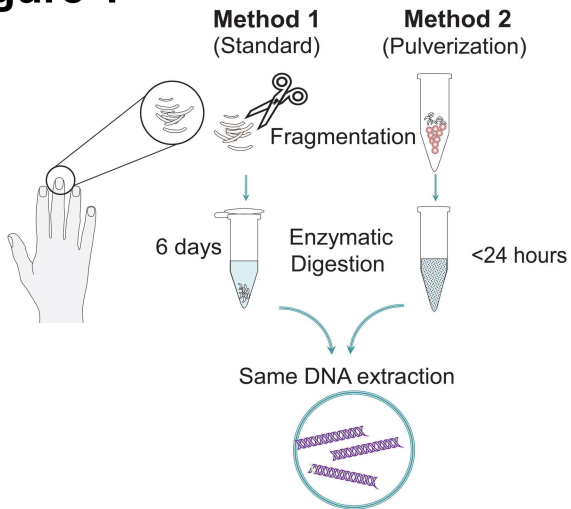
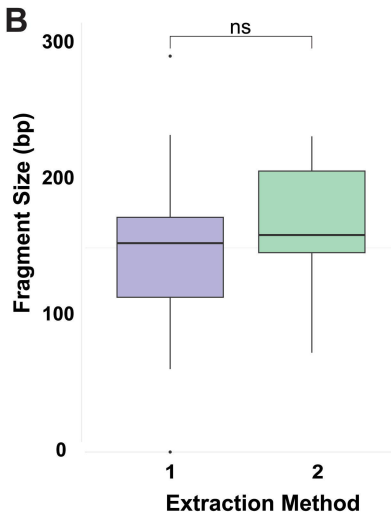
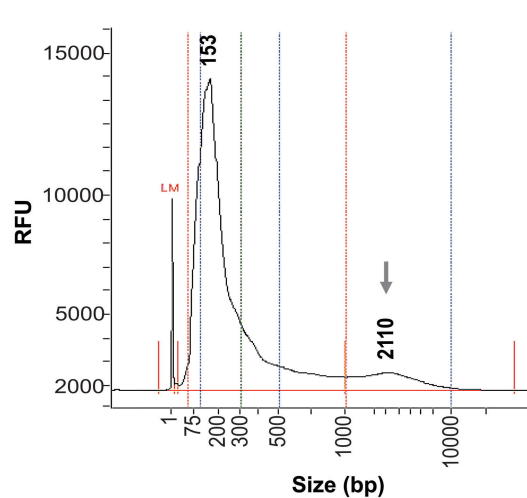
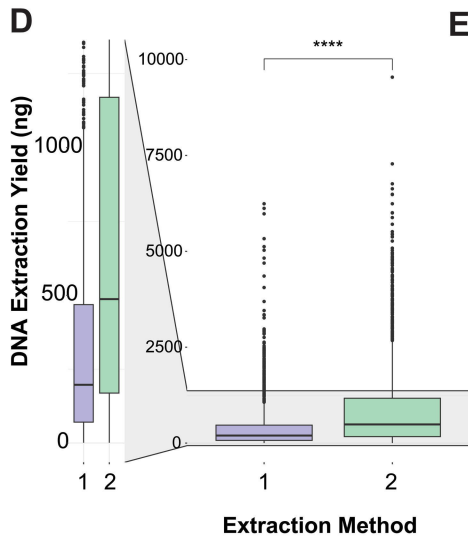
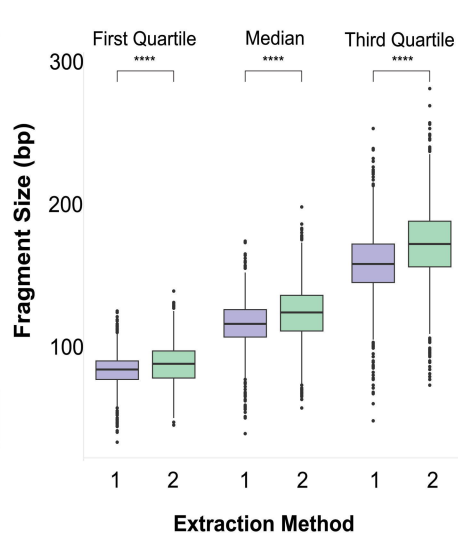
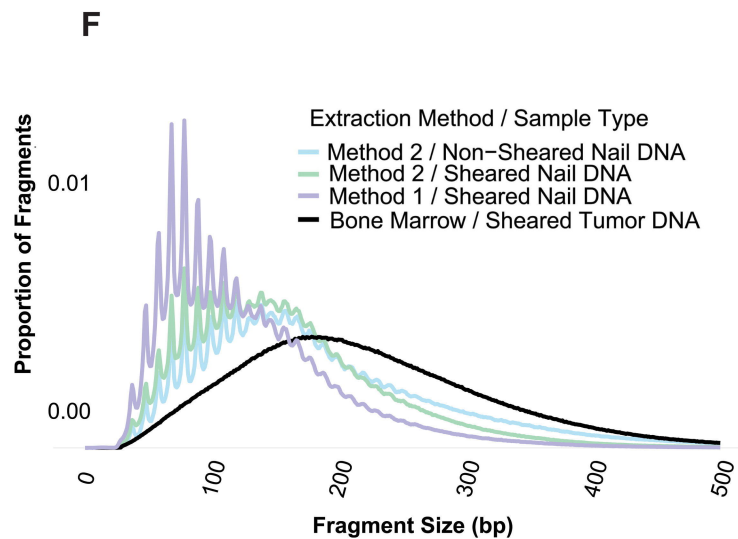
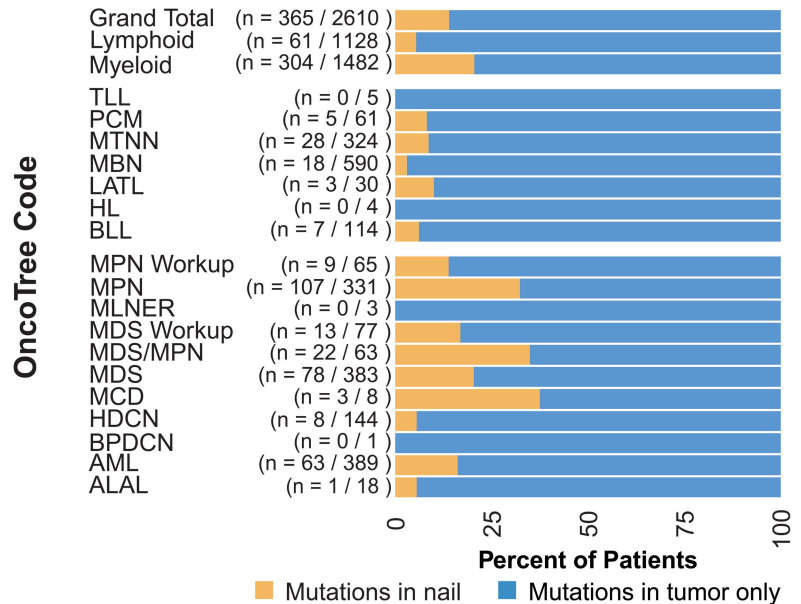
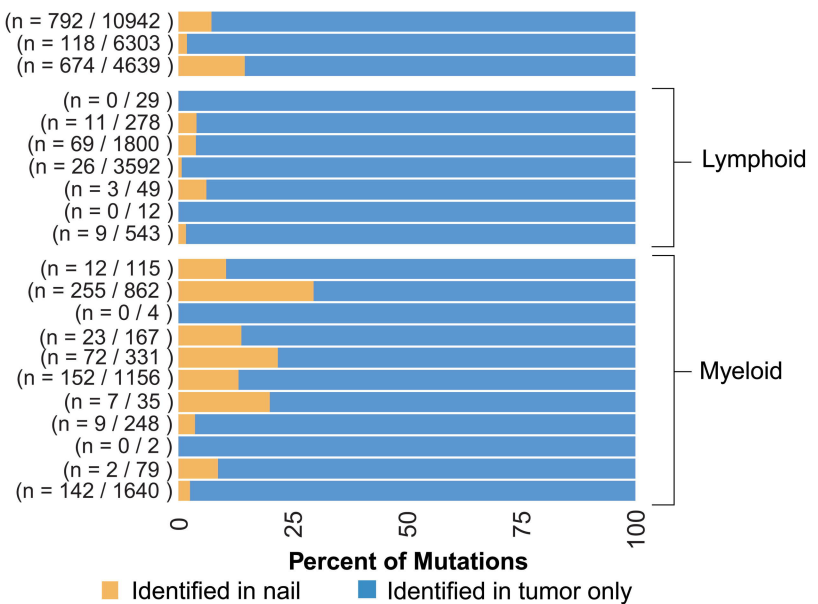
Figure 1**A****B****C****D****E****F**

Figure 2

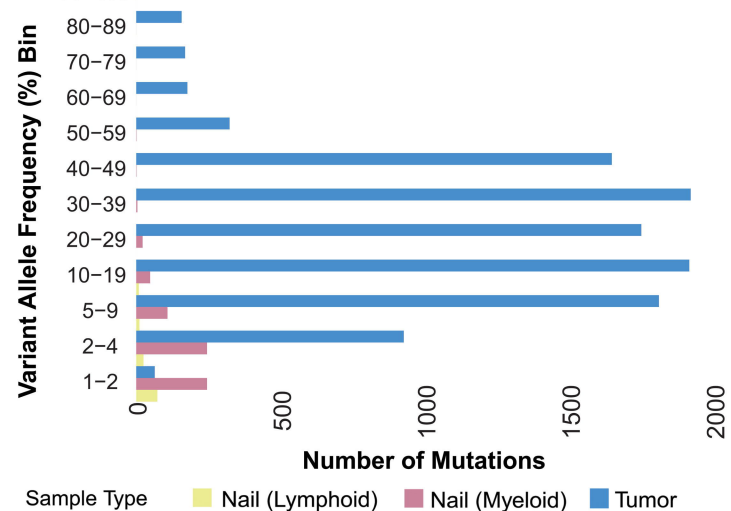
A



B



C



D

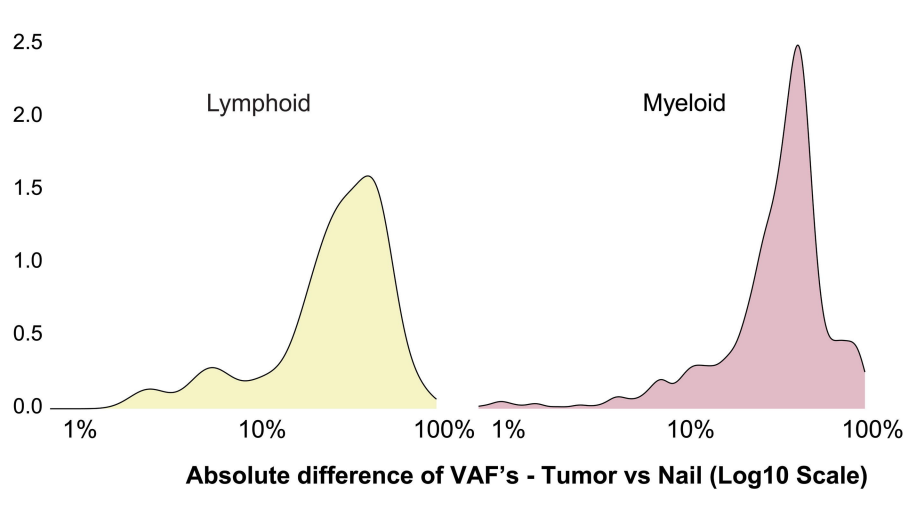
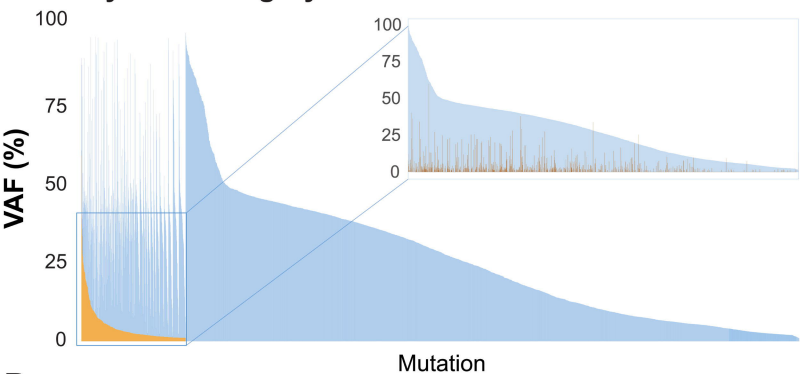
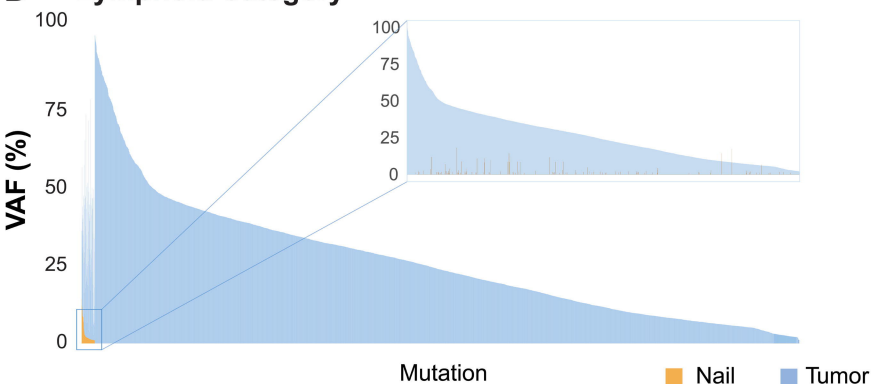
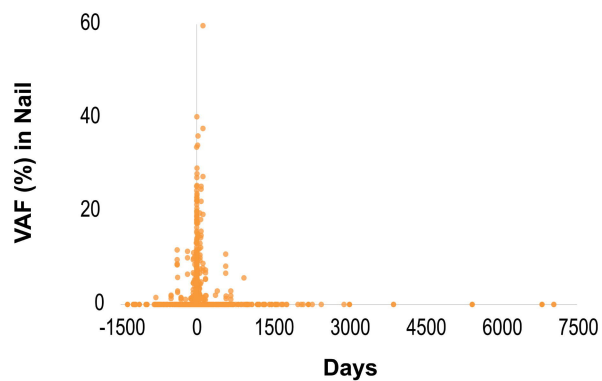
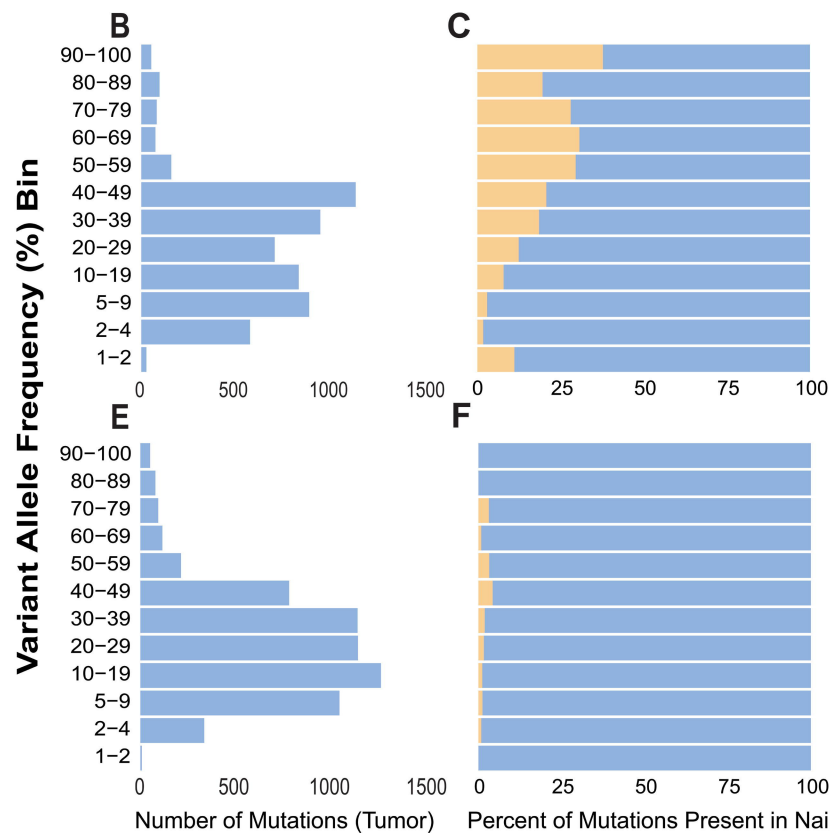
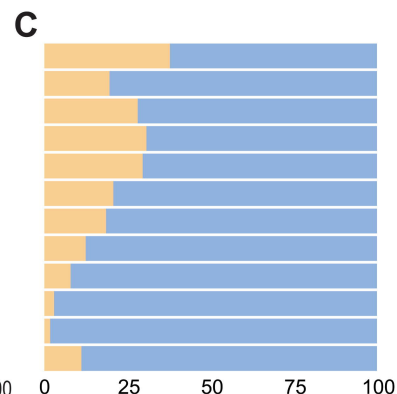
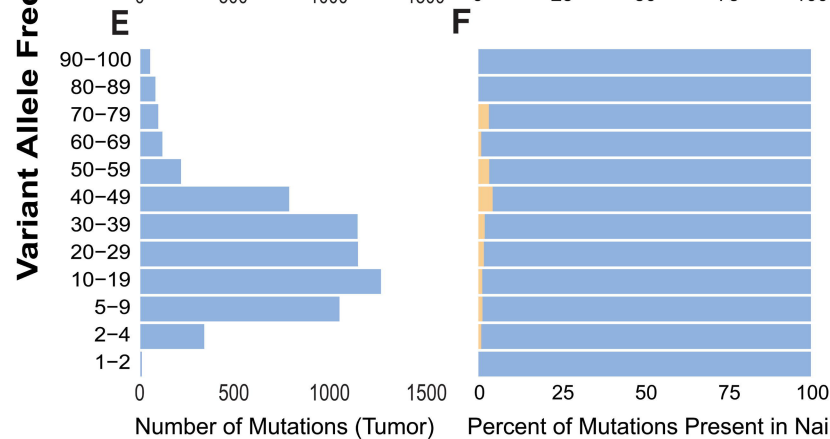
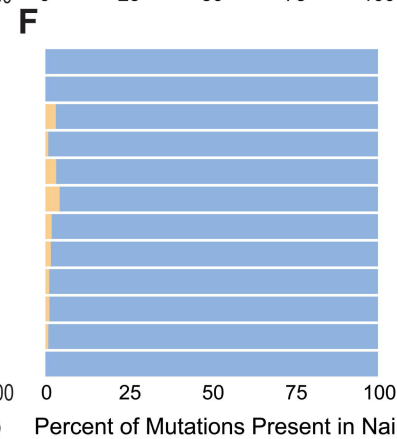
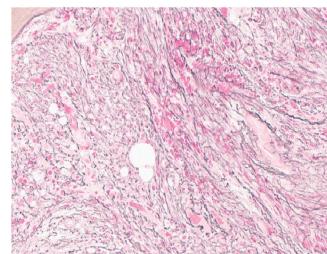


Figure 3**A Myeloid Category****D Lymphoid Category****G****B****C****E****F****H**

Gene	Mutation	VAF (%)		
		Tumor	Nail (+120 d)	Blood (+2 yr)
JAK2	p.V617F	61.3	59.7	80.6
FBXO11	p.P45_Q53del	39.5	37.7	49.6
MGA	p.V2637L	36.2	27.4	46.4
ASXL1	p.W898*	19.3	19.3	34.6
ASXL1	p.R661*	10.2	8.8	3.1
FBXO11	p.D161Y	10.7	7.8	3.0
FANCD2	p.F386V	10.8	7.2	14.3

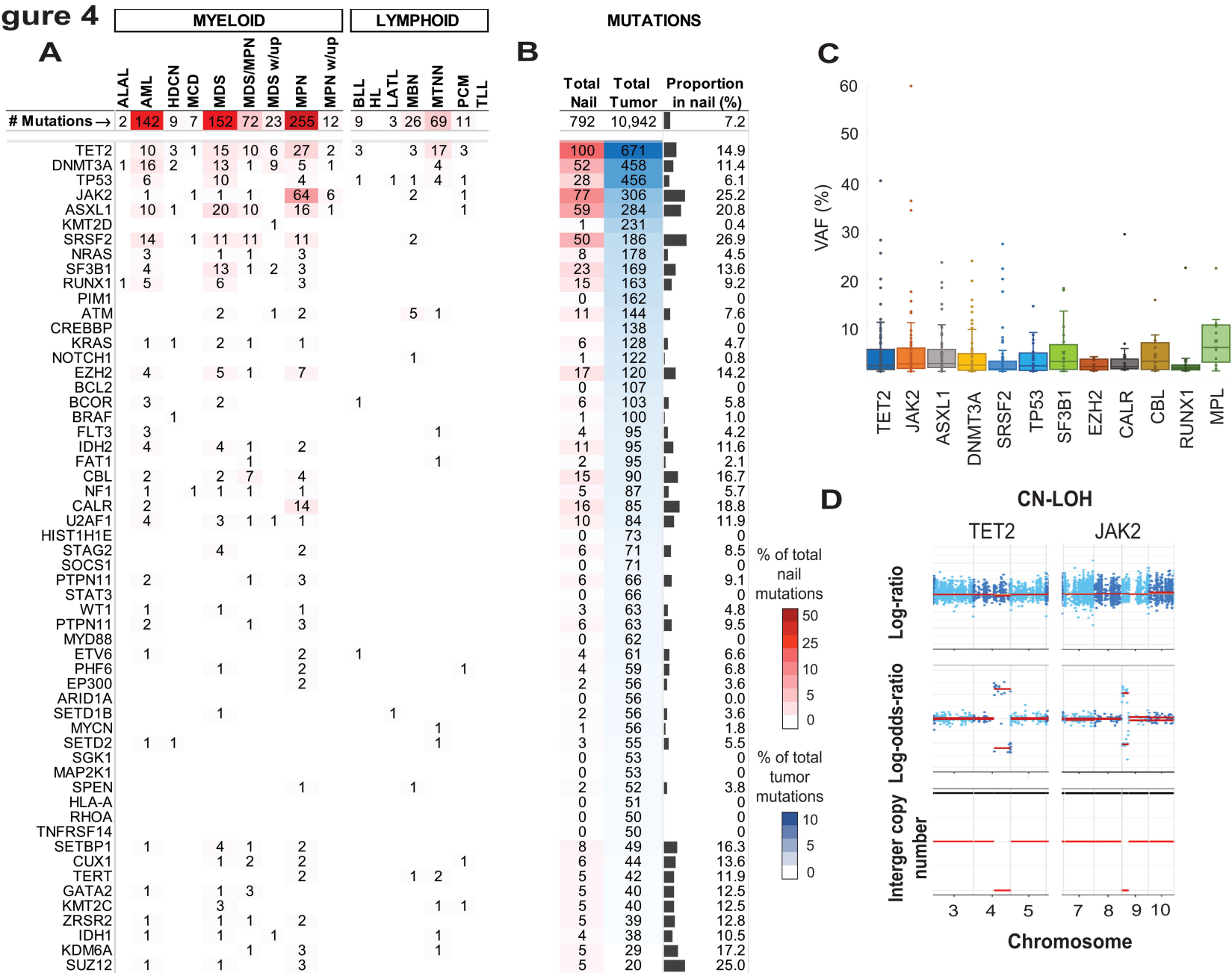
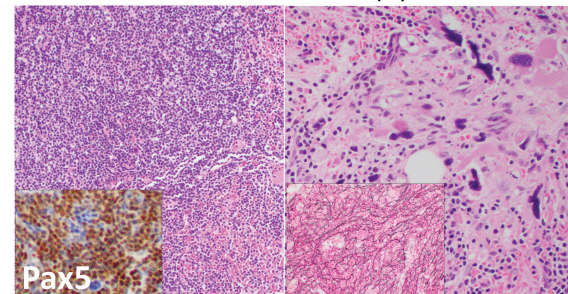
Figure 4


FIGURE 5

A CLL / SLL and Coexistent Myeloproliferative Neoplasm

	1	2	3	4	5
	Blood	Nail	BM	Sorted B	Sorted myeloid
KRAS G12D	3.7		5.5	4.4	
KRAS A146T	4.9		7.9	12.8	
NRAS G12A	1.3		2.0	3.0	
BRAF N581I	25.5		38.3	44.5	
MAP2K1 F53I	1.8		1.9	2.0	
ATM	5.4		18.8	24.9	
DDX3X	8.6		10.1	11.5	
DDX3X X500_splice	14.1		35.5	46.2	
JAK2 V617F	18.0	2.8	9.6		44.4
MPL W515L	8.2	1.0	4.0		35.6
FAT1 R3957H	9.2	2.0	4.9		24.1
NFE2 E261Afs*3	7.3	1.7	2.2		21.6
ESR1 S527N	2.0	1.0	1.0		14.6
TET2 H922Ifs*31					3.6

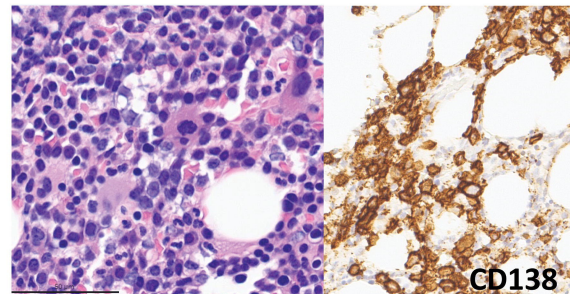
Bone marrow (3)



B Plasma Cell Neoplasm and Emerging Myelodysplastic Syndrome

	1	2	3	4	5
	BM PCM	Nail	BM PCM & MDS (1yr)	Enriched PC	BM MDS (2yr)
MGAM S459F				17.8	
PHIP S1548C				13.8	
INPP4B G558*				2.7	
SET2D G2343*				2.3	
PCBP1 L100M				2.5	
KLF2 S263F				35.6	
CDH1 P126T				5.1	
SMC3 E955*				2.4	
SPEN G574W				5.3	
NOTCH1 G310W				2.1	
RAD21 R90W				36.0	
TP53 L330I				2.4	
KRAS Q22K				22.9	
PRDM1 R9H	2.6		5.7	52.8	
TET2 E1909Dfs*39	38.1	8.5	30.2		39.5
PHF6 X244_splice	33.4	8.5	34.8		38.2
TET2 L1398Hfs*2	34.7	8.7	29.3		38.0
CUX1 X654_splice	39.5	9.6	39.3		60.3
KMT2C R2139*	35.7	11.7	31.0		42.4

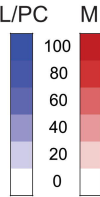
Bone marrow (3)



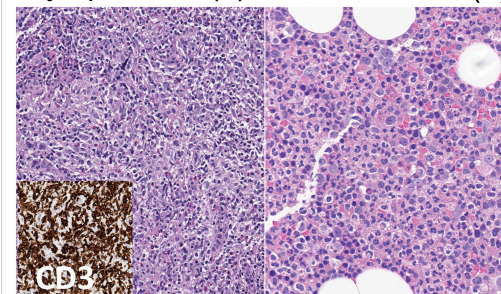
C Angioimmunoblastic T-Cell Lymphoma and Evolving MDS/MPN

	1	2	3	4
	Lymph node AITL	Nail	Blood (+6 mo)	BM (+1 yr)
HDAC4 G362A	15.4			
RHOA G17V	14.7			
IDH2 R172K	14.6			
CCND3 R271Pfs*53	13.4			
TET2 A379Vfs*6	11.5			
HGF S145G	9.0			
HLA-A X25_splice	7.6			
TET2 W1198*	45.2	18.2	81.8	79.2
DNMT3A Y724*	36.5	14.3	47.6	46.0
MYCN S369G	36.3	12.2	49.1	50.8
JAK2 V617F				38.0

NAF (%)



Lymph node (1) Bone marrow (4)



Supplementary methods section

Nail collection:

Both patient and clinicians are provided instructions on nail collection. A nail collection kit, including new nail clippers, a sterile container and a biohazard bag are provided. Nails are commonly collected in the clinics at the time of patient consent but may be collected at home following the provided instructions, when necessary. Briefly, the patient is instructed to clean their hands and nails immediately before collection. Hands are washed with soap and water, with careful attention to the nails. Nails should be free from dirt and dry prior to nail clipping. Clinicians are instructed to check nails for any unusual appearance or discoloration and, if the nails do not appear normal, collection should be avoided. Nails should be clear of any substances including, but not limited to, polish, artificial acrylic, gels, or silky overlays. Non-cosmetic substances such as dirt, residue oils, paint, ink, dyes, etc., should be removed. When removing fingernail polish prior to collection, a non-ethanol-based polish remover such as isopropyl alcohol or acetone should be used. After thorough cleaning and drying, thin slivers from the free edge (most distal end) of the nail area are collected using the nail clipper provided, avoiding collection close to the skin, and avoiding trauma or bleeding. Ten fingernail clippings are recommended.

Nail extraction:

Nail DNA extraction was performed with the QIAamp® DNA investigator kit (Qiagen), for forensic and human identity samples. Two nail fragmentation methods were used (Figure 1A): Method 1 strictly followed manufacturer's protocol. Briefly, nail clippings (2-3, ~10mg) were manually cut into 1-2mm fragments with scissors and digested overnight with Buffer ATL, proteinase K and 1M DL-Dithiothreitol Solution (DTT) (Sigma Cat. No. 646563 10X0.5 ml), at 56°C in a rotating incubator. When undigested particles were present after overnight incubation, additional proteinase K was added; the last 2 steps were repeated for several cycles (up to 6 days) to allow complete digestion. In method 2, nail clippings (~10mg) were pulverized following adjusted bone tissue protocols.(2, 3) Clippings were placed inside a 1.5ml microcentrifuge zirconium bead tube using high speed agitation and centrifugation with zirconium beads in a BeadBlaster™ 24 instrument (Benchmark Scientific, NJ) for 1 minute at a speed of 7.0M/S (miles per second). The resulting nail powder was spun down for 1 minute at 15000 RPM, followed by overnight digestion and incubation at 56°C as described above. Both methods were validated for clinical use and their side-by-side performance characteristics established through a validation set to compare

quality, yield and performance. Method 1 was used clinically from January 2017 to June 2019 and method 2 from July 2019 to December 2021.

Following DNA extraction, all samples were eluted in a 60ul volume and DNA concentration was measured by Qubit fluorometer using the dsDNA HS Assay kit (ThermoFisher Scientific/Invitrogen Cat. No. QC32854). Subsets were also analyzed by the Agilent 5300 Fragment Analyzer System with the HS Small Fragment kit (DNF-477) and the HS Genomic DNA Kit (DNF-488-1000) (Agilent, Santa Clara, CA) to assess fragment profiles, following manufacturer protocols.

Supplementary table 1 - Nail samples with time of collection >120 days of tumor sample collection						
Sample	Tumor mutations	nail mutations	Nail collection relative to tumor	OncoTree_Code	Broad disease CATEGORY	Detailed notes
P-0021485-T03-IH3	9	1	-1512	MDSWP	MDS_WORKUP	Long standing history of progressive cytopenias for 5 yrs. No workup at the time of collection as patient was diagnosed with high-grade serous carcinoma at the same time. Blood sequenced as normal control detected 5 somatic mutations (PPM1D, CBL and 3 TET2 mutations at 2-15% VAF). Bone marrow sequencing identified 9 mutations including 2 TET2, 5 TP53, PTEN and ETNK1 but morphologic assessment precluded by poor sample quality. A subsequent bone marrow sample (2 months later) was consistent with MDS-MLD 3% blasts.
P-0041336-T03-IH3	1	1	-806	PMFOFS	MPN	MPN with 3+ myelofibrosis and osteosclerosis at time of nail sampling
P-0014440-T11-IH3	3	3	-506	MDS	MDS	Myelodysplastic syndrome at the time of nail sampling. 3 mutations at low level (2-4%) but same level as tumor. Tumor sample is post transplant at time of recurrence with low level disease.
P-0047525-T02-IH3	6	5	-386	PCM	PCM	Emerging undiagnosed MDS co-occurring with PCM - case 2 in figure 5
P-0022623-T04-IH3	6	3	-376	PMF	MPN	MPN with 3+ myelofibrosis and osteosclerosis at time of nail sampling
P-0037705-T11-IH3	5	3	-309	TAML	AML	MDS/MPN at the time of nail sampling. Rapidly evolving into AML.
P-0039911-T02-IH3	3	1	-221	MDSRSMD	MDS	Myelodysplastic syndrome at the time of nail sampling. Tumor sample is post-transplant at time of recurrence with low level disease.
P-0031168-T01-IH3	4	3	-181	CMML	MDS/MPN	CMML at time of nail sampling
P-0067465-T01-IH3	2	1	153	MYCF	MTNN	Mycosis fungoides. Aggressive epidermotropic CD8+ T cell lymphoma. Extensive disease involving hands at the time of nail sampling
P-0055569-T01-IH3	8	1	171	DLBCLNOS	MBN	Refractory DLBCL. Nail collected at time of active disease. 11 alterations detected in the tumor biopsy in keeping with DLBCL - only TET2

						detected in the nail. Hypolobated megakaryocytes in marrow but no overt dysplasia. No follow up.
P-0019673-T02-IH3	5	5	173	MPN	MPN	MPN with 3+ myelofibrosis and osteosclerosis at time of nail sampling
P-0066809-T01-IH3	4	1	185	ECD	HDCN	Erdheim chester disease at time of nail sampling. Multiple mutations in tumor including ASXL1, MAP2K1 and SETD2. Only SETD2 detected in nail. Cell free DNA from plasma demonstrates active disease with detection of MAP2K1 mutation. No follow up
P-0036079-T01-IH3	4	1	369	AITL	MTNN	Angioimmunoblastic T cell lymphoma with RHOA, TET2, APC, and EZH2 mutations. Bone marrow hypercellular and left shifted myeloid maturation. No overt dysplasia. Only APC detected in nail
P-0052727-T01-IH3	2	1	406	RDD	HDCN	Rosai dorfman at time of nail sampling. Tumor shows BRAF mutation and DNMT3A. Only DNMT3A in nail. No follow up information
P-0042938-T01-IH3	15	3	570	PTCL	MTNN	PTCL involving stomach. Numerous mutations in PTCL. Only TET2, DNMT3A and GRIN2A present ~10% in nail. Patient is pancytopenic with bone marrow aplasia inconclusive for dysplasia. Died of disease before further work up.
P-0030761-T01-IH3	2	2	578	PTCL	MTNN	Peripheral T cell lymphoma. Long standing cytopenias but no diagnosis of MDS. Marrow without overt Dysplasia.
P-0026704-T03-IH3	4	3	672	AITL	MTNN	Bone marrow done for workup of thrombocytopenia - Mild atypia but no overt dysplasia. No follow up - patient died before further work up
P-0051195-T02-IH3	1	1	932	ECD	HDCN	Erheim Chester - no follow up

Table 1 includes 18 patients for whom collection of nails relative to the tumor was done beyond 4 months (120 days), before (-) or after (+).

In most cases, the patients had the same disease that was detected in the tumor. In 9 cases, the patient had active disease, similar to the tumor sample being sequenced. In 9 patients, nail mutations were CH type alterations that suggested the presence of an emerging disease myeloid disease. One patient had T cell lymphoma with extensive disease involving hands at the time of nail sampling.

Supplementary table 2: Stratification of cases by disease category – n=2610 cases

Category	Number of patients	Total Tumor Mutations	Mutations detected only in Tumor	Tumor mutations identified in Nail	Number of Patients without nail mutations	Number of Patients with nail mutations	Percent of patients with nail mutations in total cohort (n=2610)	Percent of patients with nail mutations in disease category	Percent of total mutations identified in the nail
ALAL	18	79	77	2	17	1	0.04	5.56	2.53
AML	389	1640	1498	142	326	63	2.41	16.20	8.66
BPDCN	1	2	2	0	1	0	0.00	0.00	0.00
HDCN	144	248	239	9	136	8	0.31	5.56	3.63
MCD	8	35	28	7	5	3	0.11	37.50	20.00
MDS	383	1156	1004	152	305	78	2.99	20.37	13.15
MDS/MPN	63	331	259	72	41	22	0.84	34.92	21.75
MDS WORKUP	77	167	144	23	64	13	0.50	16.88	13.77
MLNER	3	4	4	0	3	0	0.00	0.00	0.00
MPN	331	862	607	255	224	107	4.10	32.33	29.58
MPN WORKUP	65	115	103	12	56	9	0.34	13.85	10.43
BLL	114	543	534	9	107	7	0.27	6.14	1.66
HL	4	12	12	0	4	0	0.00	0.00	0.00
LATL	30	49	46	3	27	3	0.11	10.00	6.12
MBN	590	3592	3566	26	572	18	0.69	3.05	0.72
MTNN	324	1800	1731	69	296	28	1.07	8.64	3.83
PCM	61	278	267	11	56	5	0.19	8.20	3.96
TLL	5	29	29	0	5	0	0.00	0.00	0.00
Myeloid	1482	4639	3965	674	1178	304	11.65	20.51	14.53
Lymphoid	1128	6303	6185	118	1067	61	2.34	5.41	1.87
Grand Total	2610	10942	10150	792	2245	365	13.98		7.24

lymphoid categories					
MTNN and LATL	354		31	8.76	8.76
MBN AND PCM	651		23	3.53	3.53

Abbreviation key - Disease categories according to Oncotree classification

Acute Leukemias of Ambiguous Lineage (ALAL)

Acute myeloid leukemias (AML)

Blastic Plasmacytoid Dendritic Cell Neoplasm (BPDCN)

Histiocytic and Dendritic Cell Neoplasms (HDCN)

Mast cell disease (MCD)

Myelodysplastic Syndromes (MDS)

Myelodysplastic/Myeloproliferative Neoplasms (MDS/MPN)

Myelodysplastic Syndromes workup - suspected but not diagnosed (MDS workup)

Myeloid/Lymphoid Neoplasms with Eosinophilia and Rearrangement of PDGFRA/PDGFRB or FGFR1 or with PCM1-JAK2 (MLNER)

Myeloproliferative Neoplasms (MPN)

Myeloproliferative Syndromes workup - suspected but not diagnosed (MPN work up)

B-Lymphoblastic Leukemia/Lymphoma (BLL)

Hodgkin Lymphoma (HL)

Lymphoid Atypical (LATL)

Mature B-Cell Neoplasms (MBN)

Mature T and NK Neoplasms (MTNN)

Plasma Cell Myeloma (PCM)

T-Lymphoblastic Leukemia/Lymphoma (BLL)

Supplementary table 3: 19 nail samples with mutations and VAF's similar to tumor (<2 fold difference)

SAMPLE_ID	Gene	AAchange	Tumor Mutation VF	interval between nail and tumor	Broad CATEGORY	called Nail MUTATION VF	Ratio T/N	Notes
P-0007936-T06-IH3	PMS2	p.H479Q	6.4%	9	AML	9.2%	0.7	leukemia cutis
P-0026897-T01-IH3	KMT2C	p.T4218S	8.0%	19	MTNN	17.4%	0.5	PTCL with coexisting MDS. MDS mutations are subclonal in the tumor.
	TP53	p.H179Q	8.7%	19	MTNN	14.4%	0.6	
P-0030281-T04-IH3	JAK2	p.V617F	9.9%	0	MDS	5.7%	1.7	MDS with new subclonal JAK2 mutation
P-0022263-T06-IH3	MGA	p.M2780V	25.5%	64	AML	13.1%	2.0	AML with monocytic differentiation
P-0028285-T02-IH3	SRSF2	p.P95L	54.1%	3	MDS/MPN	27.2%	2.0	Bone marrow with 3+ myelofibrosis and osteosclerosis TET2 LOH
	GNB1	p.K57N	23.9%	3	MDS/MPN	14.2%	1.7	
P-0015800-T04-IH3	JAK2	p.K539L	1.0%	17	MPN	1.1%	0.9	Co-occurring CLL and MPN - 11 muts but only MPN mutations in the nail
P-0038107-T01-IH3	SF3B1	p.K700E	13.1%	13	MDS	10.2%	1.3	isolated mtuation no follow up
P-0041501-T02-IH3	TET2	p.R1216*	45.0%	87	MPN	25.3%	1.8	MDS/MPN - no marrow
	ETV6	p.A377V	49.4%	87	MPN	24.7%	2.0	MDS/MPN - no marrow
	NRAS	p.G12V	2.2%	87	MPN	1.4%	1.6	MDS/MPN - no marrow
P-0042938-T01-IH3	TET2	p.C1273Y	5.8%	570	MTNN	6.7%	0.9	PTCL involving stomach. Numerous mutations in PTCL. Only TET2, DNMT3A and GRIN2A present ~10% in nail. Patient is pancytopenic with marrow aplasia inconclusive for dysplasia. Died of disease before further work up.
P-0042185-T03-IH3	DNMT3A	p.R882H	1.0%	-10	AML	13.2%	0.1	recurrence AML low level. Nail collected at high disease level

P-0027720-T03-IH3	CALR	p.L367Tfs*46	39.3%	5	MPN	29.2%	1.3	3+ myelofibrosis and osteosclerosis TET2 LOH
	TET2	p.V1180D	40.5%	5	MPN	28.0%	1.4	
	PMS2	p.I26M	44.6%	5	MPN	25.5%	1.8	
	ASXL1	p.G646Wfs*12	36.6%	5	MPN	23.4%	1.6	
P-0014355-T13-IH3	TET2	p.N752Kfs*60	2.4%	12	MPN	1.6%	1.5	3+ myelofibrosis and osteosclerosis TET2 is subclonal in the tumor
P-0014440-T11-IH3	SRSF2	p.P95H	2.7%	-506	MDS	2.0%	1.3	myelofibrosis 2-3+ post transplant nail. Bone marrow with low level disease. Nail sample collected when blasts were 91%
	DNMT3A	p.R882H	1.6%	-506	MDS	1.3%	1.3	
P-0011024-T05-IH3	JAK2	p.V617F	61.3%	123	MPN	59.7%	1.0	Bone marrow with 3+ myelofibrosis and osteosclerosis
	FBXO11	p.P45_Q53del	39.5%	123	MPN	37.7%	1.0	
	MGA	p.V2637L	36.2%	123	MPN	27.4%	1.3	
	ASXL1	p.W898*	19.3%	123	MPN	19.3%	1.0	
	ASXL1	p.R661*	10.2%	123	MPN	8.8%	1.2	
	FBXO11	p.D161Y	10.7%	123	MPN	7.8%	1.4	
	FANCD2	p.F386V	10.8%	123	MPN	7.2%	1.5	
P-0044950-T04-IH3	DNMT3A	p.X285_splice	9.5%	-70	AML	9.6%	1.0	
P-0026778-T04-IH3	CHEK2	p.K365N	40.9%	1	MPN	24.4%	1.7	Bone marrow with 3+ myelofibrosis
	ETV6	p.H308Sfs*18	44.3%	1	MPN	22.3%	2.0	
	PTPN11	p.T73I	14.5%	1	MPN	7.4%	2.0	
P-0051394-T03-IH3	DNMT3A	p.S714C	42.9%	4	AML	23.7%	1.8	3+ myelofibrosis
	FBXW7	p.R689W	5.1%	4	AML	7.3%	0.7	
P-0053018-T03-IH3	BCOR	p.V797Lfs*10	27.8%	-3	AML	33.7%	0.8	Upper ext DVT PE double lung transplant
	U2AF1	p.S34F	18.5%	-3	AML	25.3%	0.7	
P-0066641-T02-IH3	TP53	p.N247T	2.4%	2	MDS	1.2%	2.0	no history

Supplementary Table 4 - Nail samples collected after transplant

Tumor ID	Days_from _transplant at nail collection	Status	Donor component in Nail	Evidence of GVHD (within 5 months prior to collection)	Derm notes	GVHD organ involved
P-0017576-T01-IH3	1660	N/A	Not evaluable*	No	no nail notes	
P-0008825-T08-IH3	574	CMH	42% donor	Yes	no nail notes	skin
P-0016103-T11-IH3	174	H	All host	No	no nail notes	
P-0013519-T03-IH3	426	H	All host	No	no nail notes	
P-0016085-T03-IH3	48	H	All host	No	no nail notes	
P-0014440-T11-IH3	672	H	all host (SNP)	Yes	no nail notes	UGI
P-0016588-T19-IH3	134	H	all host	No	no nail notes	
P-0009572-T13-IH3	1190	H	all host (SNP)	No	no nail notes	
P-0023500-T06-IH3	215	CMH	8% donor	No	no nail notes	
P-0031786-T02-IH3	1322	CMH	11% donor	No	no nail notes	
P-0032163-T01-IH3	1334	H	All host	No	no nail notes	
P-0032196-T01-IH3	57	CMH	10 % donor	Yes	WNL but 5 mo after	UGI/LGI
P-0032881-T07-IH3	339	H	all host	No	no nail notes	
P-0015809-T02-IH3	2689	CMH	10% donor	No (note)	no nail notes	Chronic transaminitis suggestive of chronic GVHD - no biopsy
P-0037019-T01-IH3	68	H	all host (SNP)	Yes	no nail notes	Skin
P-0037359-T01-IH3	309	H	All Host	No	no nail notes	
P-0025105-T03-IH3	125	H	SNP all host	No	no nail notes	
P-0028818-T01-IH3	2826	CMH	27% donor	Yes	no nail notes	Skin / eye
P-0020600-T06-IH3	1621	H	all host (SNP)	No	no nail notes	
P-0027574-T09-IH3	364	H	All host	No	no nail notes	
P-0042753-T01-IH3	2752	H	all host	No	no nail notes	
P-0020933-T14-IH3	504	H	all host (SNP)	No	no nail notes	
P-0043895-T01-IH3	960	H	all host (SNP)	No	no nail notes	
P-0028179-T07-IH3	356	H	all host (SNP)	No	no nail notes	
P-0034008-T04-IH3	257	H	All Host	No	no nail notes	
P-0044711-T01-IH3	2491	H	All Host	No	WNL	

P-0039015-T07-IH3	41	H	All Host	No	nail only from 1/3/2020, brittle	
P-0037562-T03-IH3	1679	H	all host (SNP)	No	no nail notes	
P-0014446-T10-IH3	918	H	all host (SNP)	No	no nail notes	
P-0034055-T04-IH3	257	H	All Host	No	no nail notes	
P-0033046-T07-IH3	132	H	All Host	No	WNL	
P-0007826-T08-IH3	1614	CMH	9% Donor	Yes	no nail notes	Liver
P-0030284-T01-IH3	1433	H	all host (SNP)	No	no nail notes	
P-0054824-T01-IH3	42	H	all host	No	no nail notes	
P-0026085-T15-IH3	855	CMH	9% donor	yes	no nail notes	Liver
P-0052508-T03-IH3	117	H	All Host	Yes	WNL	Skin
P-0056752-T01-IH3	41	H	all host (SNP)	Yes	no nail notes	UGI
P-0051949-T01-IH3	2661	H	All host	Yes	no nail notes	Eye
P-0041558-T02-IH3	3	H	all host (SNP)	No	no nail notes	
P-0034841-T07-IH3	211	CMH	15% Donor	yes	no nail notes	Skin
P-0057334-T04-IH3	307	H	All Host	No	no nail notes	
P-0016512-T13-IH3	427	CMH	14% Donor	No	no nail notes	
P-0036198-T07-IH3	3918	H	all host (SNP)	No	no nail notes	
P-0014218-T12-IH3	960	H	all host (SNP)	No	no nail notes	
P-0038787-T09-IH3	123	H	all host	no	no nail notes	
P-0031035-T16-IH3	784	H	all host (SNP)	No	no nail notes	
P-0009129-T16-IH3	1364	H	all host (SNP)	No	no nail notes	
P-0020531-T18-IH3	880	H	all host (SNP)	No	no nail notes	
P-0065092-T01-IH3	56	CMH	5% Donor	yes	no nail notes	UGI
P-0056824-T03-IH3	257	H	all host (SNP)	No	no nail notes	
P-0061278-T05-IH3	9	H	all host (SNP)	Yes	no nail notes	UGI